A SPECTROPHOTOMETRIC STUDY OF THE COMPLEXATION EQUILIBRIA AND THE DETERMINATION OF NICKEL(II) WITH 4-(2-PYRIDYLAZO)RESORCINOL, 4-(2-THIAZOLYLAZO)RESORCINOL, AND 2-(5-BROMO-2-PYRIDYLAZO)-5-(DIETHYLAMINO)PHENOL

Marie LANGOVÁ, Zdeněk ŠIMEK, Jitka CHROMÁ and Lumír SOMMER

Department of Analytical Chemistry, Purkyně University, 611 37 Brno

Received March 15th, 1986

The complexation equilibria of Ni(II) with 4-(2-pyridylazo)resorcinol (PAR) and 4-(2-thiazolylazo)resorcinol (TAR) in 30 vol.% ethanol and with 2-(5-bromo-2-pyridylazo)-5-(diethylamino)phenol (BrPADAP) in 10 vol.% ethanol containing 0·1% BRIJ-35 tenside were studied spectrophotometrically. The absorbance data were processed by the SPEFO 8, HALTAFALL SPEFO and SQUAD-G programs. The working procedures for the determination of Ni(II) with the reagents in pure solutions were optimized and statistically evaluated, and PAR was applied to the determination of Ni(II) in drinking water.

Some derivatives from the numerous class of heterocyclic azo dyes, combined with suitable masking agents and/or separation procedures for increasing selectivity, have found application in the analytical practice as highly sensitive spectrophotometric reagents for the determination of nickel in vatious materials[1]. 4-(2-Pyridylazo)-resorcinol (PAR) has been recommended for use in a number of procedures, *e.g.*, in analyses of mineral waters using ion exchangers for the separation of interfering metals[2], for the determination of nickel in Cu–Ni–Pd alloys[3], in tungsten[4], in cast iron and low-alloy steels[5], in steels after the extraction of the Ni(II)–PAR complex into ethyl acetate[6], or in crude oil making use of the extraction of the Ni(II)–PAR–tetradecyldimethylbenzylammonium bromide ternary complex into chloroform[7,8]. These procedures rely on the formation of the NiL_2^{2-} complex in weakly alkaline solutions[2,6,8–10] or $Ni(LH)_2$ complex with undissociated *p*-OH group of the ligand in weakly acid solutions[3–6]. The equilibria of Ni(II) complexes with this reagent in aqueous solutions have been evaluated by graphical analysis of spectrophotometric data[11].

4-(2-Thiazolylazo)resorcinol (TAR), a relative of PAR that is easier to synthesize, has not been so far used for the determination of Ni(II). It has been found spectrophotometrically[12] that solutions of Ni^{2+} with TAR in 30 vol.% ethanol contain complexes with the Ni : L ratios 1 : 1 and 1 : 2 and, similarly as with PAR, with the dissociated or undissociated *p*-OH group. The complexation equilibria of Ni(II) with

PAR and TAR respectively have also been studied potentiometrically in 50 vol.% dioxane[13–15]; the extraction of Ni(II) with TAR into isoamyl alcohol has been examined radiometrically[16].

2-(5-Bromo-2-pyridylazo)-5-(diethylamino)phenol (BrPADAP) is among newer, most sensitive reagents from the class of heterocyclic azo dyes. Its NiL_2 complex, similarly as its complexes with other metals[17–19], exhibits a high molar absorptivity at 560 nm, $\varepsilon = 1{\cdot}26 \cdot 10^5$ cm^2 mmol^{-1} (ref.[20]). This reagent has been recommended for the determination of nickel in aluminium alloys and electrolytic waste waters[20] and for the determination of nickel simultaneously with cobalt and copper by multicomponent spectrophotometric analysis combined with a computer evaluation[21].

In the present work, the complexation equilibria of Ni(II) with PAR and TAR are studied spectrophotometrically and evaluated numerically by means of the SPEFO 8 program on an EC 1033 computer; attention is paid particularly to systems with excess reagent, where several complexes are simultaneously formed and the conventional graphical methods, suitable for the treatment of simple isolated equilibria, fail to provide reliable results. The spectrophotometric method combined with numerical evaluation by the SQUAD-G program is also applied to the study of the complexation equilibria of Ni(II) with BrPADAP in 10 vol.% ethanol containing 0·1% BRIJ-35 tenside. The optimum conditions for the spectrophotometric determination of Ni(II) with PAR, TAR and BrPADAP are also established.

EXPERIMENTAL

Chemicals and Apparatus

4-(2-Pyridylazo)resorcinol (PAR) (Lachema, Czechoslovakia) and 4-(2-thiazolylazo)resorcinol (TAR) (prepared at the Lachema Research Institute for Pure Chemicals Brno) were purified twice prior to use. The purification routine, determination of the active component by spectrophotometric titration with copper(II) nitrate, and elemental analysis and TLC control of purity of the chemicals have been described previously[22].

2-(5-Bromo-2-pyridylazo)-5-(diethylamino)phenol (BrPADAP) (Merck, F.R.G.) was checked by elemental analysis. No colour impurities were detected by TLC.

The complexation equilibria of Ni(II) with PAR were studied in 30 vol.% ethanol in which the reagent and its nickel complexes are sufficiently soluble over the entire region of pH 1—11 (in aqueous solutions, haze appears at $c_L < 80$ μmol l^{-1} and pH 5—8). This medium was also used for TAR. For BrPADAP, haze appears shortly after mixing even in 30 vol.% ethanol, particularly at pH $\geqq$ 6. A suitable medium, in which the experiments were performed (similarly as for the BrPADAP systems with Zn(II) and Cd(II), refs[17,18]), was 10 vol.% ethanol with 0·1% BRIJ-35 or 0·3% TRITON X-100 tenside.

Stock solutions of PAR in water and TAR and BrPADAP in ethanol, prepared by dissolving weighed portions of the chemicals in the solvents, were stable for a minimum of four weeks.

Stock solution of nickel(II) nitrate, prepared from the chemical of reagent grade purity with an addition of HNO_3 (0·01 mol l^{-1}), was standardized chelometrically.

Ethanol, denatured with 5 vol.% methanol, was allowed to stand with solid EDTA and redistilled prior to use.

Polyoxyethylene monododecyl ether, $n \approx 20$, $M_r \approx 900$ (BRIJ-35) (Merck, F.R.G.), 1% stock solution was prepared by dissolving a weighed amount of the chemical in water approximately 50°C hot, allowing to cool down and diluting to volume. The solution was stable for two days at room temperature, and a week if stored in a refrigerator[17]; later a haze appeared.

Octylphenol polyethylene glycol ether, $n \approx 10$ (TRITON X-100) of analytical grade (Koch-Light, U.K.), 1% stock solution was prepared similarly as with BRIJ-35.

The acidity of the solutions for the study of the complexation equilibria of Ni^{2+} with PAR and TAR was adjusted with HNO_3 and NaOH of reagent grade purity. For BrPADAP, which is more sensitive to the presence of impurities (metal traces) in the chemicals, HNO_3 of "suprapure" grade, NaOH of "special purity" grade (Reakhim, U.S.S.R.), NH_3 of reagent grade purity additionally purified by isothermal distillation, and water redistilled in a quartz apparatus were used for these purposes and for the preparation of buffer solutions.

The absorbance–pH curves and absorption curves at various pH were measured in the continuous mode holding the ionic strength constant at $I = 0{\cdot}1$ by neutralizing the starting solution ($c_{HNO_3} = 0{\cdot}1$ mol l^{-1}) with sodium hydroxide; the volume changes were either compensated for with more concentrated solutions of the components using a glass apparatus for transferring the solution to the spectrophotometric cell[23–25], or, in a simpler arrangement, minimal volumes of concentrated NaOH solution were used for the neutralization of HNO_3 so that the total volume change over the pH region was negligible (below 0·5%). For the other absorbance dependences, the constant ionic strength ($I = 0{\cdot}1$) was maintained by adding KNO_3 recrystallized twice from a weakly alkaline medium (pH $\approx$ 9).

The absorption spectra of the solutions were scanned on a Superscan spectrophotometer (Varian, Switzerland) interfaced to a HP 9815A computer (Hewlett–Packard, U.S.A.). This equipment also allowed for recording the absorbance data for a larger set of wavelengths in a numerical form suited to further processing by the SQUAD-G program on an EC 1033 computer. The remaining absorbance dependences were measured on an SF 4A spectrophotometer (U.S.S.R.). Cells 10 mm optical path length were used.

Acidity was measured with a PHM 4d pH-meter (Radiometer, Denmark) equipped with a G 202 B glass electrode and a K 401 calomel electrode, calibrated with standard NBS buffers at pH 1·68, 4·01, 7·00 and 9·18 with an accuracy of $\pm 0{\cdot}01$ at 25°C. The pH values in solutions containing 30 vol.% ethanol or less were not corrected.

Methods of Complexation Equilibria Study

The absorbance–pH curves for the Ni(II)–PAR and Ni(II)–TAR complexes were evaluated by direct and logarithmic graphical analysis *via* slope-intercept transformations[26]. The obtained molar absorptivities and equilibrium constants converted to $\beta = [ML_nH_z]/[M]\,[L]^n\,[H]^z$ type constants were employed as the input estimates for the numerical processing of the absorbancee pH curves at one or several wavelengths (particularly at λ_{max} of the complexes) by means of the SPEKTFOT 4 program[27] in the SPEFO 8 adaptation[25,28,29]. This program seeks, for each of the successively considered complexation models, for combinations of the complex parameters such that the sum of squares of differences between the observed and calculated absorbances $U = \sum(A_{exp} - A_{calc})^2$ and the corresponding standard deviation of absorbances $\sigma(A) = \sqrt{[U/(N-p)]}$ (where N is the number of experimental values and p is the number of parameters determined) are minimum. Of the models treated, the one can be regarded as correct whose U and $\sigma(A)$ values are sufficiently low (comparable with experimental error) and so are the standard deviations $\sigma(\log \beta)$ and $\sigma(\varepsilon)$ (in the limiting case, not higher than one-third of the parameter itself[30]). The program is capable of handling parameters for as many as four complexes in the presence of no more than four other complexes with known parameters than are not varied during the calculation.

The constants and molar absorptivities so determined then were used to calculate the distribution diagrams of the complexes at selected conditions, using the HALTAFALL program[31] in the extended HALTAFALL-SPEFO modification[32,33].

The series of absorption spectra of solutions of Ni(II) with BrPADAP at different concentration ratios in dependence on pH were also evaluated by the SQUAD program[34] in the modified SQUAD-G version[35]. This program, which is based on a matrix analysis of the absorbance data for several or even a large set of wavelengths, again makes it possible, using the least squares method, to select the optimum complexation model from a number of possibilities considered and to determine the sets of ε values and equilibrium constants of the complexes formed. The program is capable of handling systems comprising as many as two different metals, two different ligands, the OH species and ten complex species .The equilibrium constants of $^*\beta = [(L_1)_p(L_2)_q \cdot (M_1)_r(M_2)_s][H^+]^t/[L_1]^p[L_2]^q[M_1]^r[M_2]^s$ type can be determined for a maximum of six complexes, the ε value sets, for all the ten complexes simultaneously. For the systems of Ni(II) ions with PAR and TAR, respectively, the absorbance data for the construction of the three-dimensional plots (response surfaces[36-38]) for the dependence of the total theoretical absorbance of the complexes (free of the reagent contribution) on pH and c_L were obtained from the known ε and $^*\beta$ values by means of the HALTAFALL-SPEFO program. The plots enabled the optimum conditions for the spectrophotometric determination of Ni(II) to be established.

RESULTS

Complexation Equilibria of Ni(II) with 4-(2-pyridylazo)resorcinol (PAR)

Acid-Base Properties of PAR

The dissociation constants of PAR in 30 vol.% ethanol at $I = 0{\cdot}1$ (KNO_3) determined by graphical and numerical analysis of the absorbance–pH curves along with the λ_{max} and ε_{max} values for the individual reagent species are given in Table I. A survey of values for various media has been given previously[39].

Absorption Spectra of Ni(II)–PAR *Complexes*

The absorption curves of Ni(II)–PAR solutions with excess reagent ($c_M = 10$ μmol . l^{-1}, $c_L/c_M = 2{\cdot}0$) and metal ($c_L = 20$ μmol l^{-1}, $c_M/c_L = 3{\cdot}1$) in 30 vol.% ethanol at pH 2·2–4·6 indicate the transition of the reagent (LH_2 and LH^-) into complex species with two absorption maxima, at 517 and 395 nm, characteristic of protonated species. At pH 5·8–10·0 the latter band vanishes and the former increases and shifts to 493 nm, which is related with the deprotonation of the initial complexes at the *p*-OH group of the bonded ligand and formation of unprotonated complexes (Fig. 1). The fractions of the complexes with M : L = 1 : 1 and 1 : 2 vary slightly in dependence on the concentrations of the components.

Method of Continuous Variations

The Job curves for the Ni(II)–PAR system in 30 vol.% ethanol at pH 2·45 ($c_0 =$

= 103 μmol l^{-1}, λ 500–530 nm), pH 4·0 (c_0 = 103 μmol l^{-1}, λ 480–530 nm) and pH 9·60 (c_0 = 18 μmol l^{-1}, λ 480–530 nm) attain their maxima at the component ratio M : L = 1 : 2.

TABLE I

Acid-base and absorption characteristics of PAR

Species	pK_a[a]	λ_{max}[b] nm	$\varepsilon_{max} \cdot 10^{-4}$[b] cm^2 $mmol^{-1}$
LH_3^+	2·66[c], 2·81[d]	395	1·60
LH_2	5·90[e], 6·30[d]	385	1·41
LH^-	13·01[f]	415	2·73
L^{2-}	—	485	2·40

[a] In 30 vol. % ethanol, I = 0·1; [b] ref.[22], aqueous solutions; [c] average of the values of pK_{a1} = = 2·65 and 2·67 found by graphical analysis for c_L = 50 μmol l^{-1} at λ 480 and 490 nm, respectively; [d] by SPEFO 8 program at c_L = 116 μmol l^{-1} and λ 520 nm; [e] average of the values of pK_{a2} = 5·89 and 5·98 found by graphical analysis for c_L = 50 μmol l^{-1} at λ 480 and 490 nm, respectively; [f] by SPEFO 8 program at c_L = 37·5 μmol l^{-1} and λ 520 nm and by graphical analysis at λ 490 and 500 nm.

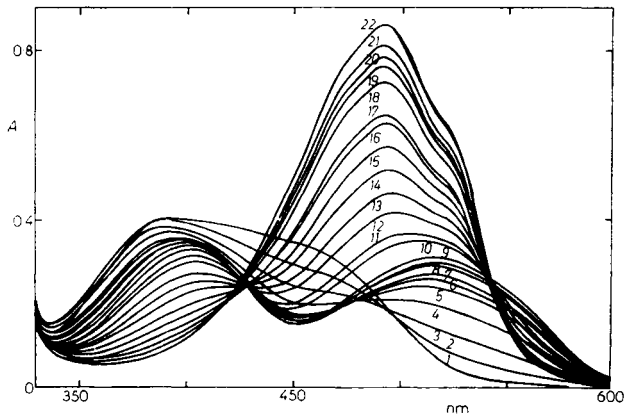

FIG. 1

Absorption spectra of solutions of Ni(II) ions with excess PAR in 30 vol.% ethanol; c_M = = 10·0 μmol l^{-1}, c_L/c_M = 2·0. pH: *1* 2·23, *2* 2·54, *3* 2·79, *4* 3·07, *5* 3·32, *6* 3·53, *7* 3·70, *8* 4·22, *9* 4·62, *10* 5·78, *11* 6·00, *12* 6·31, *13* 6·54, *14* 6·80, *15* 7·04, *16* 7·29, *17* 7·56, *18* 8·08, *19* 8·43, *20* 8·70, *21* 9·29, *22* 9·99

Concentration Dependences

The dependences $\Delta A = A - A_L = f(c_L)$ at $c_M = 10{\cdot}3$ μmol l^{-1}, pH 6·00, 6·35, 6·70 and 9·62, λ 480–530 nm, also exhibit a break at $c_L/c_M = 2{\cdot}0$. At pH 6·0–6·7, the horizontal branches decrease slightly (5–12% according to pH and λ) with respect to the value at $c_L/c_M = 2{\cdot}0$, at pH 9·62 the curve has a normal shape.

Graphical Analysis of Absorbance–pH Curves

The absorbance–pH curves at λ 500–530 nm for solutions with $c_L = 50$ μmol l^{-1} and $c_M/c_L = 50$ and 100 and the pH curves at 480–540 nm for $c_L = 25$ μmol l^{-1} and $c_M/c_L = 50$ and 100 in 30 vol.% ethanol (Fig. 2*a*, curves *1*–*4*) indicate the formation of the $NiLH^+$ complex at pH 1·0–3·8,

$$Ni^{2+} + LH_3^+ = NiLH^+ + 2\,H^+ , \qquad (A)$$

and its deprotonation to the NiL complex at pH 4·6–8·2,

$$NiLH^+ = NiL + H^+ . \qquad (B)$$

(The molar absorptivities and equilibrium constants of the two complexes are included in Table XVII.)

The absorbance–pH curves at λ 480–530 nm for solutions with $c_M = 7{\cdot}73$ μmol . . l^{-1} and $c_L/c_M = 5$ and 10 and the pH curves at λ 510–540 nm for solutions with $c_M = 15{\cdot}5$ μmol l^{-1} and $c_L/c_M = 5$ and 7·5 also have two steps associated with the formation and deprotonation of complexes with M : L = 1 : 2 (Fig. 2*b*, curves *1*–*6*).

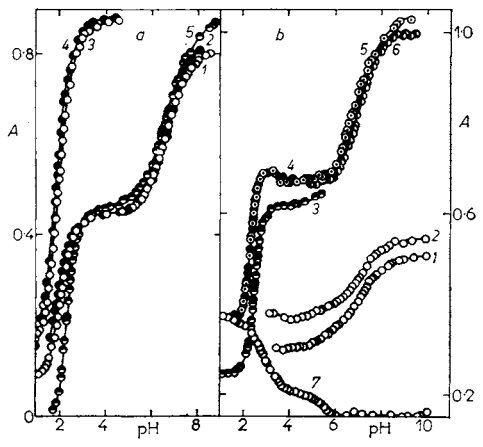

FIG. 2

Absorbance–pH curves of solutions of Ni(II) ions with PAR in 30 vol.% ethanol, λ 520 nm. *a* c_L (μmol l^{-1}), c_M/c_L: *1* 25, 50; *2* 25, 100; *3* 50, 50; *4* 50, 100. Curve *5*: $\Delta A = f$(pH) for $c_M = 15{\cdot}5$ μmol l^{-1}, $c_L/c_M = 7{\cdot}5$; *b* c_M(μ mol^{-1}), c_L/c_M: *1* 7·73, 5; *2* 7·73, 10; *3* 1·55, 5; *4* 1·55, 7·5; *5* 1·55. 7·5; *6* 1·55, 10; *7* $c_L = 165$ μ mol^{-1}, $c_M = 0$

By graphical analysis of the first branch of the pH curves at λ 520 and 530 nm, $c_M = 15{\cdot}5$ μmol l^{-1} and pH 1·8–3·5, the equilibrium

$$Ni^{2+} + 2\,LH_2 = Ni(LH)_2 + 2\,H^+ \qquad (C)$$

was identified. (The molar absorptivities and equilibrium constants of the $Ni(LH)_2$ complex are also included in Table XVII.) The analysis of the second ascending branch of these pH curves over the region of pH 5–8 failed to give the characteristics because of the simultaneous formation of several complexes. (The approximate values of the molar absorptivities of the $Ni(LH)_2$ and NiL_2 complexes determined from the horizontal segments of the pH curves at $c_M = 7{\cdot}73$ μmol l^{-1} and $c_L/c_M = 10$ as $(A - A_L)/c_M$ are also given in Table XVII).

*Numerical Analysis of Absorbance–*pH *Curves*

The absorbance–pH curves at 520 nm for excess nickel ($c_L = 50$ μmol l^{-1}, $c_M/c_L = 50$ and 100, and $c_L = 25$ μmol l^{-1}, $c_M/c_L = 50$ and 100) in 30 vol.%ethanol were first analyzed by the SPEFO 8 program assuming the occurrence of the $NiLH^+$ and NiL complexes only, and relatively low standard deviations of absorbance, $\sigma(A) = 0{\cdot}008$ to 0·013, and low standard deviations of absorptivity and complex stability constants $\sigma(\varepsilon)$ and $\sigma(\log \beta)$ were obtained. The absorbance–pH curves for excess reagent ($c_M = 15{\cdot}5$ μmol l^{-1}, $c_L/c_M = 7{\cdot}5$, and $c_M = 7{\cdot}73$ μmol l^{-1}, $c_L/c_M = 5$ and 10·5) then were evaluated using the previously established (and unvaried) ε and β values of the $NiLH^+$ and NiL complexes, and the $Ni(LH)_2$, NiL_2H and NiL_2 complexes were also detected (Table II); it was found, particularly by successive calculations of the distribution curves of the complexes by the HALTAFALL-SPEFO program for various concentrations of the components, that significant amounts of the $Ni(LH)_2$ and NiL_2H complexes and a small amount of NiL_2 were also present in solutions with excess Ni^{2+} ions. Therefore, the absorbance–pH curves for excess Ni^{2+} and for excess PAR were again treated alternately by an iteration procedure so that the $Ni(LH)_2$, NiL_2H and NiL_2 complexes with their parameters established from the curves for excess PAR were entered when processing the curves for excess Ni^{2+} (the parameters of the least abundant NiL_2 complex were held constant), and the refined values for $NiLH^+$ and NiL were again employed for a new minimization of curves with excess PAR. Ultimately, low final values of $\sigma(A)$ and refined ε and β values of the majority complexes, *i.e.*, $NiLH^+$ and NiL in solutions with excess Ni^{2+} and $Ni(LH)_2$, NiL_2H and NiL_2 in solutions with excess PAR, were thus obtained. On the other hand, higher scattering of parameter values for various data sets or higher standard deviations of the parameters were obtained for complexes formed in small amounts only, *e.g.*, for NiL at pH < 4·7 or NiL_2H and NiL_2 at pH < 5·3.

The ε and β values of the NiL_2H and NiL_2 complexes from different curves exhibit a wider range (*e.g.*, $\log \beta([NiL_2]/[Ni][L]^2) = 26{\cdot}7-27{\cdot}8$), presumably because of overlap and not very different molar absorptivities of the complexes at 520 nm ($\varepsilon(NiL_2H) = 5{\cdot}8 \cdot 10^4$, $\varepsilon(NiL_2) = 6{\cdot}3 \cdot 10^4$ cm^2 mmol^{-1}). The final ε values of the

TABLE II

The models of complexation of Ni(II) with PAR by SPEFO 8 program

Model[a]	c_L/c_M	pH[b]	$\sigma(A)$[c]	Anomalous values[d]
MLH	0·02[e]	1·0— 4·6	0·013	—
MLH, ML	0·02[e]	1·0— 4·6	0·013	—
	0·02[f]	1·7— 8·5	0·008	—
MLH, $M(LH)_2$	5·0[g]	1·1— 5·4	0·006	—
MLH, $M(LH)_2$, (ML)	0·02[e]	1·0— 4·6	0·019	—
MLH, $M(LH)_2$, ML	5·0[g]	1·1— 5·4	0·005	MLH, ML: extreme $\sigma(\varepsilon)$
	7·5[g]	1·6— 5·3	0·010	ML: enhanced $\sigma(\varepsilon)$, ε and $\sigma(\log \beta)$
MLH, ML, $M(LH)_2$, ML_2H	7·5[g]	1·6— 5·3	0·010	ML_2H: extreme $\sigma(\varepsilon)$ and $\sigma(\log \beta)$
ML, $M(LH)_2$, ML_2, (MLH)	7·5[g]	5·3—10·1	0·021	—
	10·5[h]	3·1—10·0	0·022	—
$M(LH)_2$, ML_2H, ML_2, (ML, MLH)	7·5[g]	5·3—10·1	0·006	—
	10·5[h]	3·1—10·0	0·005	—
MLH, ML, $M(LH)_2$, ML_2H, ML_2	7·5[g]	1·6— 4·3	0·008	ML_2H: extreme ε and $\sigma(\varepsilon)$ ML_2H, ML_2: enhanced $\sigma(\log \beta)$

[a] The ε and pK_a values for the LH_3^+, LH_2, LH^- and L^- species of reagent not varied during the calculation; the parameters of complexes given in parentheses, established at more suitable concentration ratios of the components, not varied either; [b] complexes with the ratio M : L = 1 : 1 prevail in the range of the first ascending branch of the absorbance-pH curves (pH 1—5·5), complexes 1 : 2 prevail in the range of the second branch (pH 5·5—10·1); for TAR the two branches overlap partly; [c] standard deviation of calculated absorbances with respect to the experimental values; [d] extremely high $\sigma(\log \beta)$ values (units to thousands) and $\sigma(\varepsilon)$ values (10^6—10)^7 indicate that the model is incorrect or that the complex is not present in an appreciable amount, enhanced $\sigma(\log \beta)$ (0·5—1·5) or $\sigma(\varepsilon)$ values (ten-thousands) with respect to the expected values also indicate a low amount of the complex in question; [e] $c_L = 50{\cdot}0$ μmol l^{-1}; [f] $c_L = 25{\cdot}0$ μmol l^{-1}; [g] $c_M =$ $= 15{\cdot}5$ μmol l^{-1}; [h] $c_M = 7{\cdot}33$ μmol l^{-1}.

various complexes determined by the SPEFO 8 program are summarized in Table III, the log β values, in Table IV.

Distribution Curves and Response Surface

The distribution curves of the Ni(II)–PAR complexes in 30 vol.% ethanol at pH 2–11 were calculated by the HALTAFALL-SPEFO program from the average stability constants determined by the SPEFO 8 program for solutions at $c_M/c_L = 100$, 1 and 0·1 (at the end of the calibration dependence). These curves (Fig. 3*a*–*c*) indicate the formation of rather complicated mixtures also in solutions for which the absorbance–pH curves (Fig. 2*a*, *b*) are apparently simple.

The response surface for the total theoretical absorbance of Ni(II)–PAR complexes at 520 nm (free of the contribution from the reagent) was obtained based on the absorbance data calculated by the HALTAFALL-SPEFO program at $c_L = 12$ to 120 μmol l^{-1} and pH 1·0–10·5. It provides an overall picture of the absorbance of

TABLE III
Molar absorptivities of complexes of Ni^{2+} with PAR at 520 nm, determined by SPEFO 8 program

c^a μmol l^{-1}	c_L/c_M	pH	$\varepsilon \pm \sigma(\varepsilon)$ 10^4 cm^2 mmol^{-1}			n^b
			NiLH	NiL		
50·3	0·02	1·0– 3·7	1·65 ± 0·01	3·7 ± 0·6[c]		31
50·0	0·01	1·2– 3·5	1·64 ± 0·01	9·4 ± 9·6		28
25·0	0·02	1·6– 8·2	1·75 ± 0·01	3·24 ± 0·02		50
25·0	0·01	1·7– 7·9	1·76 ± 0·06	3·38 ± 0·02		50
			$Ni(LH)_2$	NiL_2H	NiL_2	
15·5	5·0	1·1– 4·7	3·36 ± 0·01	7·2 ± 0·1[c]	6·5 ± 0·1[c]	46
15·5	7·5	2·1– 5·3	3·24 ± 0·02	6·0 ± 0·6[c]	3·4 ± 0·01[c]	41
15·5	7·5	1·6– 4·3	3·29 ± 0·01	5·78[d]	6·25[c]	28
15·5	7·5	5·3–10·1	3·39 ± 0·01	5·84 ± 0·01	6·22 ± 0·02	29
15·5	7·5	4·9–10·3	3·38 ± 0·01	5·91 ± 0·01	6·02 ± 0·01	44
7·73	10·5	3·1–10·0	3·53 ± 0·02	5·62 ± 0·03	6·41 ± 0·03	50
7·73	5·0	4·5– 9·9	3·55 ± 0·04	5·70 ± 0·03	6·31 ± 0·04	50
7·73	5·0[e]	4·5– 9·9	3·57 ± 0·02	5·70 ± 0·03	6·31 ± 0·04	50

[a] c_L for NiLH and NiL, c_M for $Ni(LH)_2$, NiL_2H and NiL_2; [b] number of experimental values; [c] only a negligible amount of the complex is formed at this pH; [d] average value from other results, not varied during the calculation; [e] hydrolysis equilibria of Ni^{2+}, with $\log \beta_1$ ($[NiOH][H]/[Ni]$) = = −10·2, $\log \beta_2$ ($[Ni(OH)_2][H]^2/[Ni]$) = −19·2 and $\log \beta_3$ ($[Ni(OH)_3][H]^3/[Ni]$) = −30 (ref.[40]), included in the calculation.

TABLE IV

The stability constants $\beta = [ML_nH_z]/[M][L]^n[H]^z$ of complexes of Ni^{2+} with PAR determined by SPEFO 8 program

c^a μmol l^{-1}	c_L/c_M	pH	log $\beta \pm \sigma(\log \beta)$			$\sigma(A) \cdot 10^3$
			NiLH	NiL_2		
50·3	0·02	1·0— 3·7	20·53 ± 0·01	15·4 ± 0·2[b]		11
50·0	0·01	1·2— 3·5	20·74 ± 0·02	15 ± 5.10[6b]		17
25·0	0·02	1·6— 8·2	20·35 ± 0·01	13·73 ± 0·02		6
25·0	0·01	1·7— 7·9	20·22 ± 0·01	13·44 ± 0·02		7
			$Ni(LH)_2$	NiL_2H	NiL_2	
15·5	5·0	1·1— 4·7	42·35 ± 0·01	36·49 ± 0·01[b]	26·10 ± 1·1[b]	9
15·5	7·5	2·1— 5·3	42·99 ± 0·02	36·8 ± 0·1[b]	27·0 ± 2·1[b]	13
15·5	7·5	1·6— 4·3	43·03 ± 0·03	35·63[c]	27·27[c]	11
15·5	7·5	5·3—10·1	42·27 ± 0·01	35·61 ± 0·01	27·28 ± 0·06	6
15·5	7·5	4·9—10·3	42·32 ± 0·05	35·44 ± 0·01	26·67 ± 0·08	4
7·7	10·5	3·1—10·0	42·29 ± 0·02	35·74 ± 0·02	27·78 ± 0·04	5
7·7	5·0	4·5— 9·9	42·30 ± 0·02	35·66 ± 0·02	27·42 ± 0·07	6
7·7[d]	5·0	4·5— 9·9	42·30 ± 0·02	35·66 ± 0·02	27·42 ± 0·07	6

[a] c_L for NiLH and NiL, c_M for $Ni(LH)_2$, NiL_2H and NiL_2; [b] complex present in a negligible amount at this pH (see Fig. 3*a*); [c] average value of further results, not varied during the calculation; [d] hydrolysis equilibria of Ni^{2+} included, see footnotes to Table III.

FIG. 3

Distribution curves of components in the Ni(II)–PAR system. The values of δ = = [complex]/c ($c = c_M$ for excess reagent or $c = c_L$ for excess metal) were calculated from average constants of complexes determined by SPEFO 8 program at log β (Ni + L + + H = NiLH) = 20·46, log β (Ni + L = = NiL) = 13·59, log β (Ni + 2 L + 2 H = = $Ni(LH)_2$) = 42·29, log β (Ni + 2 L + + H = NiL_2H) = 35·62 and log β (Ni + + 2 L = NiL_2) = 27·29 for c_L = 25 μmol . . l^{-1}, c_M/c_L = 100 (*a*) for $c_M = c_L$ = = 25 μmol l^{-1} (*b*) for c_M = 12 μmol l^{-1}, c_L/c_M = 10 (*c*)

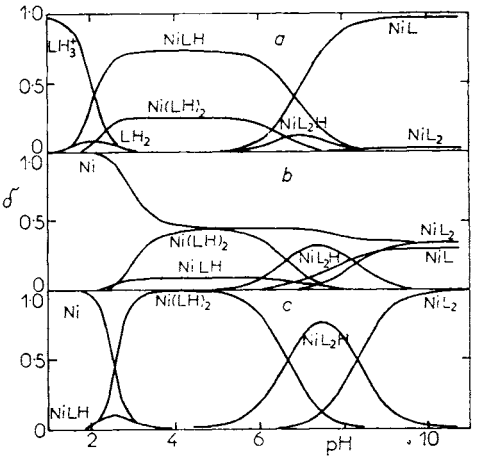

the complexes as a function of pH and c_L. The plateau in the range of $c_L/c_M = 2{\cdot}0$ and pH 9·5–11 (at pH 9·0 the absorbance is only 1% rel. lower) indicates the region suitable for the spectrophotometric determination of nickel with PAR (Fig. 4).

Spectrophotometric Determination of Ni(II) *with* PAR

In agreement with the response surface (Fig. 4), the differential absorbance–pH curves $\Delta A = A - A_L = f(\text{pH})$ for solutions with excess PAR ($c_M = 7{\cdot}73$ μmol l^{-1} and $c_L/c_M =$ = 5, 10 and 15) in 30 vol.% ethanol exhibit the highest absorbances at 480–520 nm, constant over the region of pH 9·2–10·0. The absorbance of the reagent itself is also constant in this pH range, at pH ≧ 10·0, however, it starts to increase owing to the dissociation of the *p*-OH group. The reagent concentration of $c_L = 110$ μmol l^{-1}, corresponding to the ratio of $c_L/c_M = 10$ at the end of the calibration plot, was used for the determination of nickel, although both the response surface and the concentration dependence $\Delta A = A - A_L = f(c_L)$ show that at $c_M = 8{\cdot}7$ μmol l^{-1} and pH 9·62 the reaction of Ni^{2+} with PAR is quantitative at c_L/c_M ratios as low as 2·0. According to the distribution curves, in solutions with $c_M = 12$ μmol l^{-1} and $c_L/c_M = 10$ at pH 9·2–10·0, the NiL_2 complex (λ_{max} 493 nm, $\varepsilon_{max} = 7{\cdot}96 \cdot 10^4$ cm^2 mmol^{-1}) predominates and some amount (about 6%) of the NiL_2H complex is also present (Fig. 3*c*). The spectrophotometric calibration dependence for the determination of Ni(II) with PAR was measured in 30 vol.% ethanol and also, with regard to the sufficient solubility of the reagent and its complexes in alkaline media, in aqueous solutions. The linear shape of the calibration dependence was proved by variance analysis[41]. The parameters of the calibration curve at nickel concentrations of

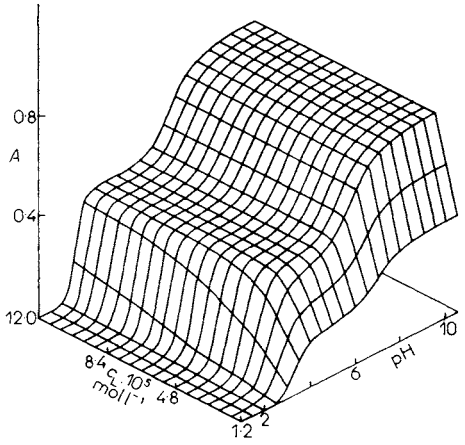

FIG. 4

Response surface for the total absorbance of complexes in the Ni(II)–PAR system at 520 nm calculated by HALTAFALL-SPEFO program from the values of constants (see text for Fig. 3) and molar absorptivities (cm^2 mmol^{-1}) of complexes at 520 nm determined by SPEFO 8 program, *viz*, ε (NiLH) = $1{\cdot}70 \cdot 10^4$, ε (NiL) = $3{\cdot}31 \cdot 10^4$. ε (Ni(LH)$_2$) = $3{\cdot}39 \cdot 10^4$, ε (NiL$_2$H) = $5{\cdot}77 \cdot 10^4$ and ε (NiL$_2$) = $6{\cdot}24 \cdot 10^4$

0·07–0·65 μg ml^{-1}, c_L = 110 μmol l^{-1} and pH 9·60 (borate buffer 0·1 mol l^{-1}) evaluated by linear regression are most favourable at λ 495 or 500 nm (see Table XIV).

Interferences from foreign ions can be suppressed by adding thiourea (0·01 mol . l^{-1}), citrate (0·2 mol l^{-1}) or EDTA (0·1 mol l^{-1}). Ti(IV) can be masked with ammonium fluoride (0·1 mol l^{-1}), UO_2^{2+} ions, with sodium carbonate (0·05 mol l^{-1}), UO_2^{2+} ions, with sodium carbonate (0·05 mol l^{-1}). Since the NiL_2 complex formation is slowed down by some competitive equilibria, it is advised to allow the solutions with the reagent to stand for 10 min. The effect of some ions on the determination of Ni(II) with PAR was tested on a system with c_{Ni} = 0·36 μg ml^{-1}, c_L = 112 μmol l^{-1}, pH 9·6 (borate buffer 0·1 mol l^{-1}), 0·01 mol l^{-1} thiourea, 0·2 mol l^{-1} tripotassium citrate and 0·1 mol l^{-1} EDTA. The limiting concentrations or interferent-to-nickel weight ratios inducing a ±2% rel. change in the absorbance of the nickel complex (after subtracting the absorbance of blank) are given in Table V.

Procedure: To a weakly acid or neutral solution of sample containing no more than 32 μg Ni placed in a 50 ml flask are added 1 ml of 0·5 ml l^{-1} thiourea solution and, after stirring, 5 ml of 0·0011 mol l^{-1} aqueous solution of PAR. The solution is allowed to stand for 10 min, 5 ml of 2 mol l^{-1} tripotassium citrate pH 9·5, 5 ml of 1 mol l^{-1} borate buffer pH 9·6 and 20 ml of

TABLE V

Effect of some ions on the determination of Ni^{2+} with PAR. Wavelength 500 nm, c_{Ni} = 0·36 μg . . ml l^{-1}, c_L = 112 μmol l^{-1}, pH 9·60 (borate buffer 0·1 mol l^{-1}) thiourea 0·01 mol l^{-1}, tripotassium citrate 0·2 mol l^{-1}, EDTA 0·1 mol l^{-1}

Ion	c_{ion}[a] μg ml^{-1}	m_{ion}/m_{Ni}[b]	Ion	c_{ion}[a] μg ml^{-1}	m_{ion}/m_{Ni}[b]
Co^{2+}	0·03	0·09	V(V)	11·0	31
Fe^{2+}	0·04	0·11	Ca^{2+}	1 270	3 527
Fe^{3+}	0·22	0·62	Mg^{2+}	1 113	3 091
Pb^{2+}	13.8	38·4	Na^{+}[c]	23 000	64 000
Cu^{2+}	21·5	59·7	K^{+}	39 000	109 000
Zn^{2+}	32·1	89·2	NH_4^{+}[c]	18 000	50 000
Mn^{2+}	52·4	146	SO_4^{2-}	2 790	7 740
Cd^{2+}	67·4	187	CO_3^{2-}	3 840	11 000
UO_2^{2+}	2·4	6·6	$H_2PO_4^{-}$	8 260	22 000
UO_2^{2+}[d]	1 890	5 261	Cl^{-}	35 000	98 500
Ti(IV)	1·4	3·9	NO_3^{-}[c]	62 000	172 000
Ti(IV)[e]	191	532	ClO_4^{-}	99 000	276 000

[a] Concentration bringing about an error of ±2% rel.; [b] mass ratio; [c] concentrations higher than 0·1 mol l^{-1} not tested; [d] in the presence of CO_3^{2-} (0·05 mol l^{-1}); [e] in the presence of F^{-} (0·1 mol l^{-1}).

0·25 mol l^{-1} EDTA pH 9·0 are added, the solution is diluted to volume and its absorbance is measured at 495 or 500 nm in 10 mm cells.

Determination of Ni(II) *in Drinking Water*

Traces of Ni(II) from drinking water, which usually contains this metal in concentrations lower than 5 ng ml^{-1}, were preconcentrated together with other metals by using the Dowex A-1 chelating ion exchanger[2] or the SPHERON–OXIN-1000 sorbent which is based on hydrophilic glycol methacrylate gels with bonded 8-hydroxyquinoline[42]. After eluting the metals from the ion exchanger with 2 mol l^{-1} HCl, traces of transition metals were trapped from the eluate in medium of 12 mol l^{-1} HCl by means of Dowex 1X8 anion exchanger, and in the solution of Ni(II) chloro complexes, nickel was determined with PAR after removing HCl by evaporation.

Metal preconcentration using Dowex A-1 *ion exchanger.* Sample of 1 000 ml of drinking water with a standard addition of 18·1 μg Ni^{2+} and 1 ml of concentrated HNO_3 to preserve hydrolysis was adjusted to pH ≈ 6·5 with ammonia, passed through a 9·5 cm long column 12 mm in diameter of Dowex A-1, grain size 50—100 mesh, in the Na^+ cycle; the solution flow rate was 3·5 ml min^{-1}. The column then was washed with 30 ml of redistilled water, Ni(II) and other metals were eluted with 50 ml of 2 mol l^{-1} HCl at a rate of 0·5—1·0 ml min^{-1}, and the eluate was evaporated to dryness.

Metal preconcentration using SPHERON-OXIN-1000 *sorbent.* To 1 000 ml of drinking water were added a standard addition of Ni^{2+}, 1 ml of concentrated HNO_3, ammonia to a neutral reaction and acetate buffer (0·01 mol l^{-1}) pH 5·0. One g of sorbent was added and the system was agitated for 2 h. The sorbent was then separated, washed with 20 ml of redistilled water and eluted with 30 ml of 2 mol l^{-1} HCl and 10 ml of redistilled water, and the solution was evaporated to dryness.

Separation of Ni(II) *from interfering metals on Dowex* 1X8 *anion exchanger.* The evaporation residue from the metal preconcentration was dissolved in 2 ml of 12 mol l^{-1} HCl and applied to a Dowex 1X8 column 10 cm long, 0·8 cm in diameter, pretreated with 12 mol l^{-1} HCl. The solution of 12 mol l^{-1} HCl used before for rinsing the sample residues from the dish then was also applied, and the anion exchanger was eluted with 30 ml of 12 mol l^{-1} HCl at a flow rate of 0·5—0·7 ml min^{-1}. The eluate in a quartz dish was evaporated to dryness and the residue was dissolved in 10 ml of redistilled water and transferred to a 50 ml volumetric flask for the determination of Ni(II) with PAR. The relative error of determination of Ni(II) in drinking water derived from three replicate analyses of water with a standard addition of 363 μg Ni^{2+} *per* litre of water and a model sample with the ratio of Ni : Cu : Co = 1 : 2 : 0·5, using the preconcentration procedure with Dowex A-1, was −3·0 to −5·2% rel., the error of determination of three parallel samples with the same addition of nickel, using the preconcentration on SPHERON-OXIN-100, lay within the limits of +4·1 to +5·8% rel.

Complexation Equilibria of Ni(II) with 4-(2-Thiazolylazo) resorcinol (TAR)

Acid-Base Properties of TAR

The dissociation equilibria of TAR in 30 vol.% ethanol have been studied in detail previously[12,22]; they comprise transitions of the following species:

LH_3^+ with λ_{max} 481 and pK_{a1} ($[LH_2][H^+]/[LH_3^+]$) = 0·75 (I = 1·0),
LH_2 with λ_{max} 438 nm and pK_{a2} ($[LH^-][H^+]/[LH_2]$) = 6·51 (I = 0·1),
LH^- with λ_{max} 480 nm and pK_{a3} ($[L^{2-}][H^+]/[LH^-]$) = 10·67 (I = 0·1), and
L^{2-} with λ_{max} 513 nm.

The partial data found in this work graphically and using the SPEFO 8 program for our particular conditions (pH, c_L, λ) of study of the complexation equilibria of Ni(II) with TAR, *viz.* pK_{a2} = 6·51, $\varepsilon(LH_2)$ = 327 cm^2 mmol^{-1} and $\varepsilon(LH^-)$ = 3·51 . . 10^3 cm^2 mmol^{-1} at 540 nm, agree with the results[39,22]; the pK_{a1} and ε values of the LH_3^+ species at I = 0·1, only serving for small corrections during the numerical treatment of the complexation equilibria, were evaluated from a short segment the pH curve of TAR over the region of pH 1·0–3·9.

Absorption Spectra of Ni(II)–TAR *Complexes*

The absorption curves of solutions of Ni^{2+} with a small excess of reagent (c_M = = 15·5 μmol l^{-1}, c_M/c_L = 2·0) in 30 vol.% ethanol exhibit over the range of pH 3·06 to 5·18 two maxima at 540 and 420–430 nm corresponding to the formation of the NiLH and $Ni(LH)_2$ protonated species, and at pH 6·6, a maximum at 505 mn corresponding to their deprotonation to the NiL and NiL_2H chelates (Fig. 5). Previously[12] the absorption curves of solutions of TAR with excess Ni^{2+} (c_M/c_L = 70) over the region of pH 1·8–7·7, and solutions of TAR with increasing concentration of Ni^{2+} at pH 3·1 and pH 8·0 were measured, from which the absorption maxima of the $NiLH^+$

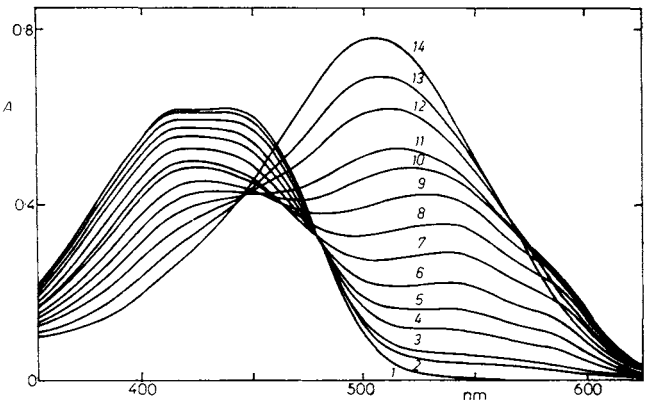

FIG. 5

Absorption spectra of solutions of Ni(II) ions with excess TAR in 30 vol.% ethanol; c_M = = 15·5 μmol l^{-1}, c_L/c_M = 2·0. pH: *1* 3·06, *2* 3·92, *3* 4·10, *4* 4·38, *5* 4·56, *6* 4·77, *7* 5·00, *8* 5·18, *9* 5·39, *10* 5·59, *11* 5·89, *12* 6·06, *13* 6·25, *14* 6·65

complex at 536 and 415 nm and the absorption maximum of the NiL complex at 505 nm were evaluated, and the occurrence of a mixture of complexes with M : L = = 1 : 1 and 1 : 2 at pH 4·3–5·6 and of a complex 1 : 2 at pH 7·5–8 was established by the variation method.

*Graphical Analysis of Absorbance–*pH *Curves*

The first ascending branch of the absorbance–pH curves at λ 500 and 540 nm for solutions of TAR with excess Ni^{2+} (c_L = 25·0 μmol l^{-1}, c_M/c_L = 100 and 200, and c_L = 40·0 μmol l^{-1}, c_M/c_L = 100 and 200) in 30 vol.% ethanol over the pH 2·0–4·5 range (Fig. 6*a*) were subjected to graphical analysis[26] and the equilibrium

$$Ni^{2+} + LH_2 = NiLH^+ + H^+ \qquad (D)$$

was identified. The analysis of the second branch of the pH curves at λ 500 nm for c_L = 25·0 μmol l^{-1} and c_M/c_L = 100 and 200 at pH 5·0–7·0 gave evidence of the deprotonation of the complex formed,

$$NiLH^+ = NiL + H^+ . \qquad (E)$$

(The equilibrium constants and molar absorptivities of the $NiLH^+$ and NiL complexes are included in Table XVII.)

The absorbance–pH curves of solutions of Ni^{2+} with excess reagent (c_M = = 16·0 μmol l^{-1}, c_L/c_M = 5, and c_M = 12·0 μmol l^{-1}, c_L/c_M = 8·5, Fig. 6*b*) gave no linear dependences for the $Ni(LH)_2$ complex at pH 4·5 or for its deprotonation at pH > 5 because of a simultaneous formation of several complexes.

*Numerical Analysis of Absorbance–*pH *Curves*

Similarly as for the Ni(II)–PAR system, the $NiLH^+$, NiL, $Ni(LH)_2$, NiL_2H^- and NiL_2^{2-} complexes were identified based on the numerical processing of the absorbance–pH curves of Ni(II)–TAR systems both with excess Ni^{2+} (c_L = 40·0 μmol l^{-1}, c_M/c_L = 100 and 200, and c_L = 25·0 μmol l^{-1}, c_M/c_L = 100 and 200) and with excess TAR (c_M = 16·0 μmol l^{-1}, c_L/c_M = 5, and c_M = 12·0 μmol l^{-1}, c_L/c_M = 8·5, 10 and 15) (Table VI).

The pH curves of solutions of TAR with excess Ni^{2+} at pH 1·5–5·1 provided reliable values of the stability constant and molar absorptivity for the $NiLH^+$ complex, and over a wider region of pH 1·7–7·9, values of the parameters for both the $NiLH^+$ and NiL complexes. Complexes with the Ni : L = 1 : 2 ratio are formed in very low quantities in these circumstances (Fig. 7*a*), and therefore the values of their parameters exhibit a higher variance and higher standard deviations. For the

complexes given above, more reliable values were derived from the curves for the system with excess TAR where these complexes predominate (Fig. 7*c*). The stability constants of the type of $[ML_nH_z]/[M][L]^n[H^+]^z$ and molar absorptivities at 540 nm determined by the SPEFO 8 program are given in Tables VII and VIII, respectively.

Distribution Curves and Response Surface

The distribution curves of Ni(II)–TAR complexes in 30 vol.% ethanol at pH 2·8–8·8 calculated by the HALTAFALL-SPEFO program from the average stability constants obtained by the SPEFO 8 program (Fig. 7*a–c*) show the relative amounts of complexes for the concentration ratios c_M/c_L = 100, 1 and 0·2.

The response surface of the total absorbance of the complexes in dependence on pH over the region of pH 1–9·5 and on the concentration of reagent over the region of c_L = 25–253 μmol l^{-1}, obtained based on the absorbances calculated by the HALTAFALL-SPEFO program from the stability constants and molar absorptivities

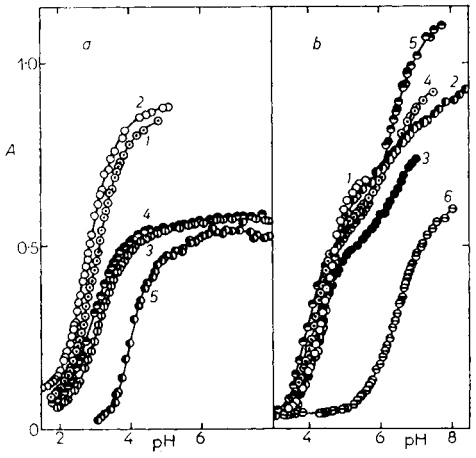

FIG. 6

Absorbance–pH curves of solutions of Ni(II) ions with TAR in 30 vol.% ethanol, λ 540 nm. *a* c_L (μmol l^{-1}), c_M/c_L: *1* 40, 100; *2* 40, 200; *3* 25, 100; *4* 25, 200. Curve *5*: $\Delta A = f(\text{pH})$ for c_M = 12 μmol l^{-1}, c_L/c_M = 15. *b* c_M μmol l^{-1}), c_L/c_M: *1* 16, 5·0; *2* 16, 5·0; *3* 12, 8·5; *4* 12, 10; *5* 12, 15; *6* c_L = 18 μmol l^{-1}, c_M = 0

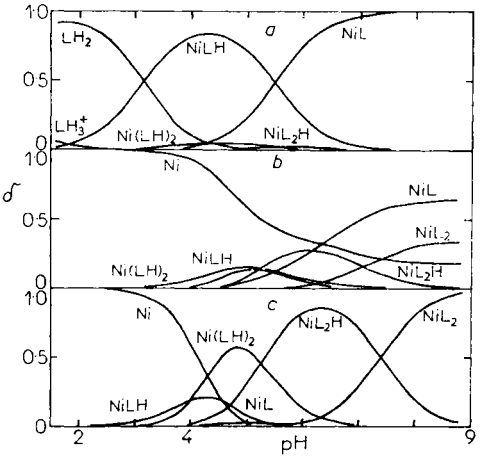

FIG. 7

Distribution curves of components in Ni(II)–TAR system (see text for Fig. 3) calculated at log β (Ni + L + H = NiLH) = 16·57, log β (Ni + L = NiL) = 11·08, log β (Ni + 2 L + 2 H = $Ni(LH)_2$) = 33·66, log β (Ni + 2 L + H = NiL_2H) = 28·64 and log β (Ni + 2 L = NiL_2) = 21·03 for c_L = 25 μmol l^{-1}, c_M/c_L = 100 (*a*), c_M = c_L = 25 μmol l^{-1} (*b*) and c_M = 25 μmol l^{-1}, c_L/c_M = 5·0 (*c*)

at 540 nm determined by the SPEFO 8 program (Fig. 8) exhibits the maximum constant absorbances at pH 8·5–9·5 and $c_L = 61$ μmol l^{-1}.

Spectrophotometric Determination of Ni(II) *with* TAR

With regard to the high absorbance of the reagent in weakly alkaline solutions ($\varepsilon_{540} = 3{\cdot}51 \cdot 10^3$ and $2{\cdot}00 \cdot 10^4$ cm^2 mmol^{-1} for the LH^- ($pK_{a3} = 10{\cdot}67$) and L^{2-} species, respectively) the pH 6·0–7·0 range was selected for the determination of nickel, although according to the response surface patterns (Fig. 8) the absorbance increases slightly with pH in this range. The experimental absorbance–pH curves $\Delta A = A - A_L = f$ (pH) for $c_M = 16{\cdot}0$ μmol l^{-1}, $c_L/c_M = 5$, and $c_M = 13{\cdot}0$ μmol . l^{-1}, $c_L/c_M = 15$ exhibit virtually constant absorbances at 530 and 540 nm in this pH region and absorbances at 550 and 560 nm even slightly decreasing from pH 5·5; some distortion of the differential curves, however, may be due to the fact that the total, non-constant absorbance of reagent was subtracted. According to distribution

TABLE VI
The models of complexation of Ni(II) with TAR by SPEFO 8 program

Model[a]	c_L/c_M	pH[b]	σ(A)[c]	Anomalous values[d]
MLH, ML	0·02[e]	1·8–7·9	0·003	–
	0·01[e]	1·9–7·9	0·003	
	0·005[f]	1·5–5·1	0·005	ML: enhanced σ(log β)
	8·5[g]	2·1–7·0	0·057	
$M(LH)_2$, (MLH, ML)	8·5[g]	3·1–7·0	0·007	–
ML_2H, (MLH, ML)	15[g]	3·6–7·8	0·048	–
ML_2, (MLH, ML)	10[g]	3·6–7·5	0·049	–
$M(LH)_2$, ML_2H, (MLH, ML)	8·5[g]	3·1–7·0	0·012	$M(LH)_2$: low ε
$M(LH)_2$, ML_2, (MLH, ML)	10[g]	3·6–7·5	0·004	–
	8·5	3·1–7·0		
MLH, ML, $M(LH)_2$, ML_2H, (ML_2)	0·005[e]	1·8–7·9	0·003	$M(LH)_2$: σ(ε)
	0·01[e]	1·9–7·9	0·003	$M(LH)_2$: enhanced σ(log β) and σ(ε)
	0·005[f]	1·5–5·1	0·005	ML_2H: enhanced σ(log β) and σ(ε)
$M(LH)_2$, ML_2H, ML_2, (MLH, ML)	5·0[h]	3·1–8·4	0·007	–
	8·5[g]	3·1–7·0	0·003	–
	10[g]	3·6–7·5	0·007	–

[a,b,c,d] As in Table II; [e] $c_L = 2{\cdot}5$ mmol l^{-1}; [f] $c_L = 40{\cdot}0$ μmol l^{-1}; [g] $c_M = 12{\cdot}0$ μmol l^{-1}; [h] $c_M = 16{\cdot}0$ μmol l^{-1}.

diagram (Fig. 7*c*), the absorbance changes in this pH range are a consequence of the occurrence of equilibria of complexes of various degrees of protonation, the NiL_2H^- complex predominating in the presence of lower amounts of $Ni(LH)_2$ and NiL_2^{2-}. At the same time, the absorbance of reagent increases because of its dissociation;

TABLE VII

Molar absorptivities of complexes of Ni^{2+} with TAR at 540 nm determined by SPEFO 8 program

c^a / μmol l^{-1}	c_L/c_M	pH	$\varepsilon \pm \sigma(\varepsilon)$ / 10^4 cm^2 mmol^{-1}			n^b
			NiLH	NiL		
40·0	0·01	1·8—4·8	2·15 ± 0·02	2·27 ± 0·04[c]		39
40·0	0·005	1·5—5·1	2·20 ± 0·01	2 ± 12[c]		43
25·0	0·01	1·9—7·9	2·16 ± 0·01	2·30 ± 0·01		50
25·0	0·005	1·7—7·9	2·18 ± 0·01	2·33 ± 0·01		50
			$Ni(LH)_2$	NiL_2H	NiL_2	
16·0	5·0	3·4—4·5	4·31 ± 0·01	4·15 ± 0·04	6·59	28
16·0	5·0	3·1—8·4	3·02 ± 0·04	4·15 ± 0·01	4·73 ± 0·04	47
12·0	8·5	3·0—7·0	3·04 ± 0·02	4·03 ± 0·01	233	48
12·0	10	3·6—7·5	3·68 ± 0·03	4·96 ± 0·02	6·59 ± 0·2	50
12·0	15	3·6—7·8	3·78 ± 0·06	4·86 ± 0·03	5·92 ± 0·3	50

[a] c_L for NiLH and NiL, c_M for $Ni(LH)_2$, NiL_2H and NiL_2; [b] number of experimental values; [c] a small amount of NiL complex and negligible amounts of 1 : 2 complexes (see Fig. 7*a*).

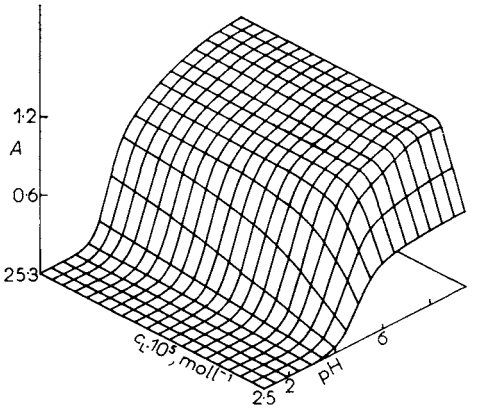

FIG. 8

Response surface of total absorbance of complexes in Ni(II)–TAR system at 540 nm (see text for Fig. 3) calculated for the constants as in Fig. 7 and molar absorptivities (cm^2 mmol^{-1}) ε (NiLH) = 2·18 . 10^4, ε (NiL) = 2·32 . 10^4, ε ($Ni(LH)_2$) = 3·57 . . 10^4, ε (NiL_2H) = 4·43 . 10^4 and ε (NiL_2) = = 5·75 . 10^4

therefore, the determination of Ni(II) with TAR at pH 6·0–7·0 requires a precise pH adjustment.

When investigating the effect of reagent, a quantitative formation of complexes starting from $c_L/c_M = 5$ was deduced from the $\Delta A = f(c_L)$ dependence at $c_M =$ $= 16{\cdot}0\ \mu mol\ l^{-1}$ and pH 6·50. The reagent concentration $c_L = 130\ \mu mol\ l^{-1}$ was chosen for the determination, *i.e.*, $c_L/c_M \approx 5$ at $c_M = 25\ \mu mol\ l^{-1}$ at the end of the calibration dependence.

The acidity of the solutions for the determination of Ni(II) can be adjusted with ammonium acetate, which at pH 6·5 does not interfere up to a concentration of $0{\cdot}3\ mol\ l^{-1}$, or with triethanolamine–HNO_3 or phosphate buffers, which do not interfere up to a concentration of $0{\cdot}15\ mol\ l^{-1}$ at pH 6·5 and pH 6·6, respectively. The results are unaffected by the ionic strength up to $I = 0{\cdot}5$ (KNO_3). The spectrophotometric calibration region of $c_{Ni} = 0{\cdot}12-1{\cdot}45\ \mu g\ ml^{-1}$ at pH 6·48 (ammonium acetate $0{\cdot}2\ mol\ l^{-1}$) and $c_L = 130\ \mu mol\ l^{-1}$ in 30 vol.% ethanol, measured at λ 535, 540, 545 and 550 nm and 10 mm optical path length was subjected to linear regression calculations. The parameters at 540 or 545 nm were confirmed as the most suitable (see Table XIV).

TABLE VIII

The stability constants $\beta = [ML_nH_z]/[M]\,[L]^n\,[H]^z$ of complexes of Ni^{2+} with TAR determined by SPEFO 8 program

c^a / μmol l^{-1}	c_L/c_M	pH	log $\beta \pm \sigma(\log \beta)$			$\sigma(A) \cdot 10^3$
			NiLH	NiL		
40·0	0·01	1·8–4·8	16·55 ± 0·01	11·07 ± 0·08[b]		2
40·0	0·005	1·5–5·1	16·48 ± 0·01	7·5 ± 1261[b]		5
25·0	0·01	1·9–7·9	16·66 ± 0·01	11·09 ± 0·04		2
25·0	0·005	1·7–7·9	16·58 ± 0·01	11·07 ± 0·04		3
			$Ni(LH)_2$	NiL_2H	NiL_2	
16·0	5·0	3·4–5·5	33·59 ± 0·04	28·29 ± 0·03	21·00[c]	8
16·0	5·0	3·1–8·4	33·55 ± 0·02	28·78 ± 0·01	21·29 ± 0·07	7
12·0	8·5	3·0–7·0	33·46 ± 0·01	28·85 ± 0·05	18·04 ± 0·15[d]	3
12·0	10·0	3·6–7·5	33·87 ± 0·02	29·00 ± 0·01	21·00 ± 0·05	7
12·0	15·0	3·6–7·8	33·81 ± 0·03	28·26 ± 0·07	20·81 ± 0·09	10

[a] c_L for NiLH and NiL, c_M for $Ni(LH)_2$, NiL_2H and NiL_2; [b] a small amount of NiL and negligible amounts of 1 : 2 complexes (see Fig. 7*a*); [c] values from $c_L/c_M = 10$, not varied; [d] a small amount of NiL_2.

Complexation Equilibria of Ni(II) with 2-(5-Bromo-2-pyridylazo)-5-(diethylamino)phenol (BrPADAP)

Acid-Base Properties of BrPADAP

The dissociation of BrPADAP in the region of nickel complexation, pH 2·0–12·8, in 10 vol.% ethanol in the presence of 0·1% BRIJ-35 tenside was evaluated from the absorption curves of solutions of BrPADAP (c_L = 33·4 μmol l^{-1}, EDTA 0·1 mmol . . l^{-1} for suppressing the effect of metal traces) with increasing pH, by graphical analysis[26] at 500 and 510 nm, and by numerical analysis of a set of absorbance data for 24 wavelengths within the 380–580 nm region using the SQUAD-G program[35]. The pK_a, λ_{max} and ε_{max} values of the LH_2^+, LH and L^- species at I = 0·1 ($NaNO_3$) and 25°C are given in Table IX.

For the LH_3^{2+} species formed in strongly acid solutions, the pK_{a1} values found recently in 50 vol.% ethanol were 0·1 ± 0·1 (ref.[43]) and 0·05 (ref.[44]), in 30 vol.% ethanol, −0·29 (ref.[44]).

A survey of dissociation constants and absorption data of BrPADAP in various media can be found in refs[19,44], where the order of protonation of the reagent substituents is also discussed: the pK_{a3}, pK_{a2} and pK_{a1} values are attributed to the phenolic group, the pyridine nitrogen atom and the diethylamino group, respectively, whereas in ref.[43] the protonation of the pyridine nitrogen and the diethylamino group is assumed to proceed in the reverse order.

Absorption Spectra of Ni(II)–BrPADAP *Complexes*

The absorption spectra of solutions of BrPADAP with excess Ni^{2+} (c_L = 16·4 μmol . . l^{-1} and c_M/c_L = 100) in 10 vol.% ethanol in the presence of 0·1% BRIJ-35 at pH 2·0–6·0 indicate the transition of the reagent (the LH_2^+ and LH species, λ_{max} 445 nm at pH ≈ 2) into a product with a double maximum at 525–552 nm and in isosbestic point at 480 nm (Fig. 9). The curves for the system with excess reagent (c_M = 3·60 μmol l^{-1} and c_L/c_M = 4·64) at pH 2·6–6·4 exhibit a gradually appearing partly resolved double maximum at 525–559 m (Fig. 10). The same λ_{max} values and the isosbestic point at 485 nm were observed for BrPADAP solutions with increasing concentration of Ni^{2+} (c_L = 16·8 μmol l^{-1} and c_M/c_L = 0·1–1·0) at pH 8·8. The different shapes of the double maxima at different concentration ratios of the components suggest that at least two complexes with different Ni : L ratios are formed.

Continuous Variations Method

Only the complex with Ni : L = 1 : 2 was detected by the continuous variations method in solutions of Ni^{2+} with BrPADAP in 10 vol.% ethanol in the presence of

0·3% TRITON X-100 tenside at pH 2·80 (c_0 = 43·8 μmol l^{-1}) and at pH 3·75 and 8·50 (c_0 = 33·0 μmol l^{-1}), λ 525, 540, 560 and 570 nm.

Absorbance–pH Curves

The absorbance–pH curves at 525–560 nm for c_M = 7·20 μmol l^{-1}, c_L/c_M = 4·64; c_M = 6·00 μmol l^{-1}, c_L/c_M = 100; and c_L = 16·3 μmol l^{-1}, c_M/c_L = 100, in 10 vol.% ethanol in the presence of 0·1% BRIJ-35 (Fig. 11) or 0·1% TRITON X-100 have a single monotonically ascending branch over the region of pH 2–5; this simple shape, however, does not rule out a simultaneous formation of a larger number of complexes.

TABLE IX

Acid-base and absorption characteristics of BrPADAP in 10 vol.% ethanol containing 0·1% BRIJ-35, I = 0·1

Species	pK_a	λ_{max} nm	$\varepsilon \cdot 10^{-4}$ cm^2 mmol^{-1}
LH_2^+	2·33 ± 0·04[a], 2·28[b], 2·32[c]	463	4·23
LH	11·43[b], 11·41[c]	443	4·07
L^-	—	512	4·69

[a] Calculated by SQUAD program for 24 wavelengths within the region of 380–480 nm; [b] obtained by graphical analysis at 500 nm; [c] obtained by graphical analysis at 510 nm.

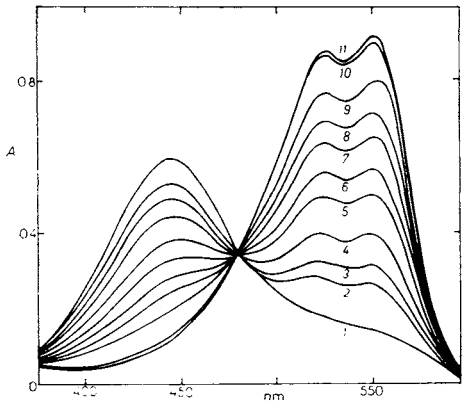

FIG. 9

Absorption spectra of solutions of BrPADAP with excess Ni(II) ions in 10 vol.% ethanol containing 0·1% BRIJ-35 tenside; c_L = 16·3 μmol l^{-1}, c_M/c_L = 101. pH: *1* 2·02, *2* 2·69, *3* 2·85, *4* 3·04, *5* 3·25, *6* 3·40, *7* 3·57, *8* 3·77, *9* 4·00, *10* 4·90, *11* 6·00

Numerical Treatment of Absorption Curves

Several sets of absorbance data at 22 wavelengths within the region of 380–580 nm (step 10 nm and λ 525 nm in addition) for $c_L = 16{\cdot}4\ \mu mol\ l^{-1}$, $c_M/c_L = 101$, and $c_M = 7{\cdot}19\ \mu mol\ l^{-1}$, $c_L/c_M = 4{\cdot}64$ and 9·98, in 10 vol.% ethanol in the presence of 0·1% BRIJ-35 at pH 2–6 were treated by the SQUAD-G program. Only the data at 560 nm, *i.e.* in the absorption maximum range, were used for the SPEFO 8 treatment. Various models involving the ML, ML_2, MLH, $M(LH)_2$ and ML_2H complexes were considered (Table X). For systems with excess reagent, the U, $\sigma(A)$, $\sigma(\varepsilon)$ and $\sigma(\log \beta)$ data along with other criteria obtained by the two programs suggest the ML_2 + ML complex pair as the most adequate. The ε and $\log \beta$ values of the NiL_2 complex and, in particular, the NiL complex determined by the SQUAD-G program, however, exhibit a considerably higher variance than those determined by the SPEFO 8 program (Tables XI and XII), presumably as a manifestation of the law of propagation of errors for data at wavelengths more distant from the maximum of the complexes, where the errors of measurement, inaccuracies in the high absorbances of reagent, effect of aggregation, formation of colloids of reagent and complexes, *etc.*, can play a significant part as compared to the low changes in the absorbances of the complexes.

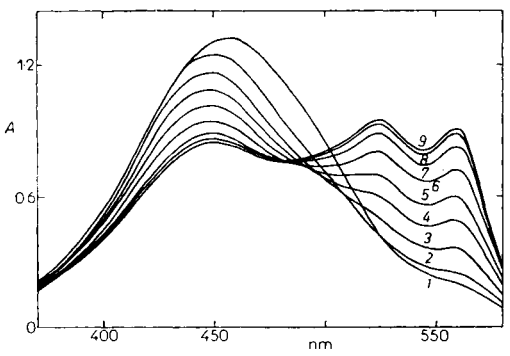

FIG. 10

Absorption spectra of solutions of Ni(II) ions with excess BrPADAP in 10 vol.% ethanol containing 0·1% BRIJ-35; $c_M = 7{\cdot}20\ \mu mol\ l^{-1}$, $c_L/c_M = 4{\cdot}64$. pH: *1* 2·14, *2* 2·61, *3* 2·93, *4* 3·16, *5* 3·37, *6* 3·68, *7* 4·10, *8* 4·88, *9* 5·49

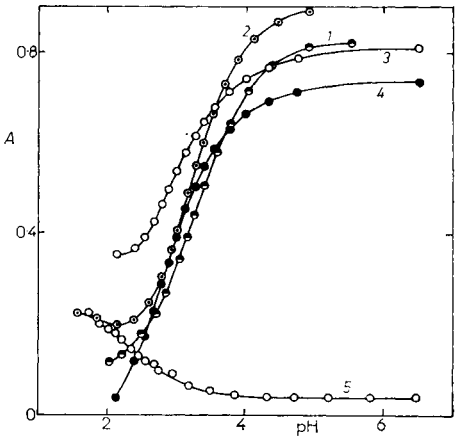

FIG. 11

Absorbance–pH curves of solutions of Ni(II) ions with BrPADAP in 10 vol.% ethanol containing 0·1% BRIJ-35, 560 nm. *1* $c_L = 16{\cdot}4\ \mu mol\ l^{-1}$, $c_M/c_L = 101$; *2* $c_M = 6{\cdot}00\ \mu mol\ l^{-1}$, $c_L/c_M = 10$; *4* $\Delta A = f(pH)$ for $c_M = 6{\cdot}00\ \mu mol\ l^{-1}$, $c_L/c_M = 10$; *5* $c_L = 33{\cdot}4\ \mu mol\ l^{-1}$, $c_M = 0$

TABLE X

The Ni(II)–BrPADAP complexation models by SQUAD-G and SPEFO 8 programs

Model[a]	c_L/c_M[b]	$\sigma(A)$[c]	Anomalous values[d]
		SQUAD-G	
ML_2	4·64	0·009	—
	9·98	0·055	—
ML_2, ML	4·64	0·003, 0·019[e]	—
	9·98	0·007	—
$M(LH)_2$	4·64	0·087	$\sigma(\log\beta)$, ε
	9·98	0·061	$\sigma(\log\beta)$, ε
ML_2, ML, MLH	4·64	0·003	MLH: $\sigma(\log\beta)$, ε[f]
	4·64	0·027[e]	MLH: $\sigma(\log\beta)$, ε
	9·98	0·006	MLH: $\sigma(\log\beta)$, ε
ML_2, ML, $M(LH)_2$	4·64	0·004	$M(LH)_2$: $\sigma(\log\beta)$, ε ML: $\varepsilon < 0$
ML_2, ML_2H, $M(LH)_2$	4·64	0·078	all complexes: $\sigma(\log\beta)$, ML_2: ε, $M(LH)_2$: $\varepsilon < 0$
ML_2, ML, MLH, ML_2H	4·64	0·003[e]	all complexes: $\sigma(\log\beta)$, ML: ε, ML_2H: $\varepsilon < 0$
	9·98	0·019	all complexes: $\sigma(\log\beta)$, ML, MLH, ML_2H: ε
ML_2, ML, MLH, ML_2H, $M(LH)_2$	4·64	0·011	ML, MLH: $\log\beta$,
	9·98	0·007	except ML_2: ε
		SPEFO 8	
ML_2	4·64	0·029, 0·034[e]	—
	9·98	0·047	—
ML_2, ML	4·64	0·002, 0·001[e]	—
	9·98	0·006	—

[a] ε and pK_a values of LH_2^+ and LH species not varied during calculation; [b] $c_M = 7{\cdot}20$ μmol l^{-1} for $c_L/c_M = 4{\cdot}64$, $c_M = 6{\cdot}00$ μmol l^{-1} for $c_L/c_M = 9{\cdot}98$; and $c_L = 16{\cdot}3$ μmol l^{-1} for $c_L/c_M = 0{\cdot}009$ [c] standard deviation of calculated absorbances with respect to the experimental data at the same wavelength; [d] extremely high, nonreal $\sigma(\log\beta)$ values (units to thousands), extremely high ε and $\sigma(\varepsilon)$ values (10^5—10^6) or negative ε give evidence of incorrectness of the model treated or a low amount of the complex in question; [e] acidity (pH 2·8—4·4) adjusted with ammonia, otherwise with sodium hydroxide for systems with $c_L/c_M = 4{\cdot}64$ (pH 2·0—4·6) and $c_L/c_M = 9{\cdot}98$ (pH 2·1—4·7); [f] computation terminated after 11 iterations, for the remaining anomalous results the calculation did not converge and was discontinued after 25 iterations.

From the data set for excess Ni(II) (c_M/c_L = 101) neither of the programs provided ε and β parameters of the ML_2 and ML complexes identical with those for excess reagent along with a low U criterion, not even after augmenting the ML_2 + ML system with the MLH and M_2L complexes.

The distribution curves of the Ni(II)–BrPADAP complexes calculated by the HALTAFALL-SPEFO program from the more accurate average parameters of the complexes determined by the SPEFO 8 program for solutions with excess reagent (c_L/c_M = 4·64 and 9·98) at pH 2·0–5·0 are shown in Fig. 12.

TABLE XI

Values of molar absorptivities of Ni(II)–BrPADAP complexes at 560 nm determined by means of SQUAD-G (SQ) and SPEFO 8 (SP) programs

c_L/c_M	pH	$\varepsilon \pm \sigma(\varepsilon) \cdot 10^4$ cm^2 mmol^{-1}				$\sigma(A)$[a]	
		NiL		NiL_2		SQ	SP
		SQ	SP	SQ	SP		
4·64[b]	2·0–4·6	2·06 ± 0·08	4·60 ± 0·03	11·98 ± 0·04	11·86 ± 0·02	0·003	0·002
4·64[b]	2·5–5·1	6·73 ± 0·16	5·06 ± 0·11	12·00 ± 0·07	12·02 ± 0·04	0·020	0·006
4·64[b,c]	2·8–4·5	1·97 ± 0·05	4·44 ± 0·02	11·92 ± 0·02	11·98 ± 0·01	0·019	0·001
9·98[d]	2·1–4·7	3·49 ± 0·04	5·20 ± 0·09	11·26 ± 0·07	11·64 ± 0·06	0·007	0·006

[a] Standard deviation of calculated absorbances with respect to the experimental values; number of solutions measured see in Table XII; [b] c_M = 7·20 μmol l^{-1}; [c] pH adjusted with ammonia, otherwise with sodium hydroxide; [d] c_M = 6·00 μmol l^{-1}.

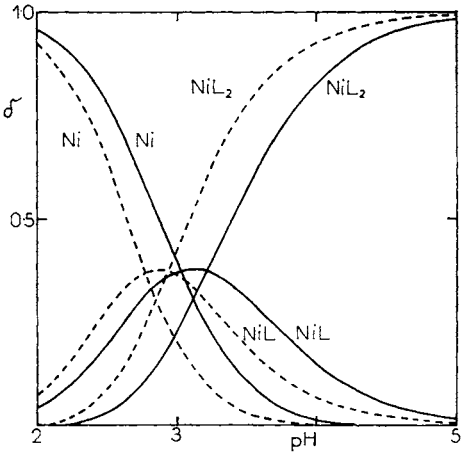

FIG. 12

Distribution curves of complexes in Ni(II)–BrPADAP system. The distribution coefficients (δ), $[NiL_2]/c_M$, $[NiL]/c_M$ and $[Ni]/c_M$ calculated by HALTAFALL-SPEFO program using log β(Ni + 2 L = NiL_2) = 25·90, and log β (Ni + L = NiL) = 13·04, determined by SPEFO 8 program, for c_M = 7·20 μmol l^{-1}, c_L/c_M = 4·64 (full lines) and c_M = 6·00 μmol l^{-1}, c_L/c_M = 10 (dashed lines)

TABLE XII

Values of constants of Ni(II)–BrPADAP complexes determined by means of SQUAD-G (SQ) and SPEFO 8 (SP) programs

c_L/c_M [a]	NiL			NiL_2			
	$\log {}^*\beta \pm \sigma(\log {}^*\beta)$ [b] SQ	$\log \beta$ [c] SQ	$\log {}^*\beta \pm \sigma(\log {}^*\beta)$ [d] SP	$\log {}^*\beta \pm \sigma(\log {}^*\beta)$ [b] SQ	$\log \beta$ [c] SQ	$\log {}^*\beta \pm \sigma(\log {}^*\beta)$ [d] SP	N [e]
4·64	−0·39 ± 0·06	13·36	13·03 ± 0·01	−1·20 ± 0·08	26·30	25·94 ± 0·003	15
4·64	−0·91 ± 0·09	12·84	12·99 ± 0·004	−2·00 ± 0·19	25·50	25·91 ± 0·01	9
4·64	−0·57 ± 0·19	13·18	13·01 ± 0·01	−1·30 ± 0·25	26·20	25·93 ± 0·003	11
9·98	+0·33 ± 0·05	14·08	13·13 ± 0·02	−0·61 ± 0·05	26·89	25·82 ± 0·01	15

[a] c_M values and pH adjustment as in Table XI; [b] ${}^*\beta = [NiL_p][H]^{2p}/[Ni][LH_2]^p$ from data at 22 wavelengths; [c] $\beta = [NiL_p]/[Ni][L]^p$ calculated from ${}^*\beta$ as $\beta = {}^*\beta/K_{a2}^p K_{a3}^p$ ($pK_{a2} = 2{\cdot}33$, $pK_{a3} = 11{\cdot}42$); [d] at 560 nm; [e] number of solutions measured at 22 wavelengths (380–580 nm) for SQUAD-G treatment and at 560 nm for SPEFO 8 treatment.

Spectrophotometric Determination of Ni(II) *with* BrPADAP

Ni(II) can be determined with BrPADAP in the form of the NiL_2^{2-} complex with λ_{max} 560 and 525 nm, $\varepsilon_{560} = 1{\cdot}21 \cdot 10^5$ cm^2 mmol^{-1}, in 10 vol.% ethanol containing 0·1% BRIJ-35 at pH 6·5–9·0 and $c_L = 84$ μmol l^{-1} ($c_L/c_M = 10$ at the end of the calibration curve). According to the course of the concentration dependence $\Delta A = A - A_L = f(c_L)$ for the Ni^{2+}–BrPADAP system at $c_M = 6{\cdot}0$ μmol l^{-1} and pH 6·5 and 8·8, and according to the calibration dependences (Table XIII), the concentration of BrPADAP can be lowered with increasing pH in this region, *viz.* to $c_L = 67$ μmol l^{-1} at pH 8·0 ($c_L/c_M = 8$) and $c_L = 50$ μmol l^{-1} at pH 8·8–9·0 ($c_L/c_M = 6{\cdot}5$ at $c_M = 8{\cdot}35$ μmol l^{-1} in pure solutions free from interferents), whereby the risk of appearance of haze is lowered. The acidity can be adjusted with ammoniacal buffer which does not interfere up to a concentration of 0·3 mol l^{-1} at pH 8·8, or tris(hydroxymethyl)aminomethane which does not interfere up to a concentration of 0·4 mol l^{-1} at pH 8·9, or borate buffer which does not interere up to a concentration of 0·1 mol l^{-1} at pH 9·0. The differences in the slopes of the calibration curves for these buffers at different pH and c_L values lie within the limits of random error (Table XIII). Ionic strength does not affect the absorbance up to $I = 1{\cdot}0$ ($NaNO_3$) in conditions suitable for the determination.

Procedure: To a slight acid to neutral solution of sample containing no more than 12 μg Ni, placed in a 25 ml volumetric flask, are added 2·5 ml of 1% aqueous solution of BRIJ-35, 2·5 ml of 840 μmol l^{-1} ethanolic solution of BrPADAP and 2·5 ml of 2·0 mol l^{-1} TRIS buffer (pH 7·5), the solution is diluted to volume with water and the absorbance is measured at 560 nm in 10 mm cells.

The characteristics of the calibration curve for the spectrophotometric determination over the nickel concentration region of 0·05–0·49 μg ml^{-1}, calculated by linear regression after testing the linearity by variance analysis[41], are given in Table XIV. The effect of some ions on the determination is shown in Table XV, the effect of some conventional masking agents, also in mixtures, in Table XVI. A simultaneous presence of thiourea (final concentration 0·2 mol l^{-1}), tartrate (0·2 mol l^{-1}), fluoride (0·08 mol l^{-1}) and EDTA (2·0 mmol l^{-1}), however, proved inefficient for masking Fe(III), Cu(II) and Co(II).

DISCUSSION

In Ni(II)–PAR and Ni(II)–TAR systems in 30 vol.% ethanol, the $NiLH^+$, NiL, $Ni(LH)_2$, NiL_2H^- and NiL_2^{2-} complex species were identified. The average values of their constants and molar absorptivities are summarized in Table XVII.

The NiL_2H^- complexes have never been before detected spectrophotometrically, except for the complex with PAR (ref.[11]), because they are formed simultaneously with the $Ni(LH)_2$ and NiL_2^{2-} species from which they do not differ significantly

TABLE XIII

Slopes of spectrophotometric calibration dependences for the Ni(II)–BrPADAP system at 560 nm; $c_M = 0{\cdot}8-8{\cdot}35$ μmol l^{-1}, medium: 10 vol.% ethanol containing 0·1% BRIJ-35

Buffer	pH	c_L μmol l^{-1}	$\varepsilon \cdot 10^{-5}$ cm^2 mmol^{-1}	A_0[a]
—	9·00	54	1·184	0·074
TRIS 0·2 mol l^{-1} [b]	8·95	54	1·158	0·099
	8·10	67	1·183	0·117
NH_3 0·2 mol l^{-1}	9·02	54	1·176	0·080
Borate 0·1 mol l^{-1} [c]	9·02	54	1·173	0·094
TEA 0·1 mol l^{-1} [d]	7·00	84	1·247	0·094
Acetate 0·06 mol l^{-1} [e]	5·50	84	1·186	0·077

[a] Absorbance of blank solution; [b] at pH 7·2 and $c_L = 84$ μmol l^{-1} time instability and haze in 40 min; [c] at pH 8·2 and $c_L = 67$ μmol l^{-1} bending of calibration dependence starting at $c_M = 6{\cdot}68$ μmol l^{-1}; [d] medium 30 vol.% ethanol; in 10 vol.% ethanol with 0·1% BRIJ-35 at $c_L = 84$ μmol l^{-1} time instability both in the presence of 0·1 mol l^{-1} triethanolamine at pH 7·2 and of 0·1 mol l^{-1} phosphate buffer at pH 6·75; [e] conditions according to ref.[20], medium of 30 vol.% ethanol.

TABLE XIV

Parameters of spectrophotometric calibration curves for determination of Ni(II) with PAR, TAR and BrPADAP determined by linear regression

Reagent	λ nm	$b \cdot 10^{-4}$ [a] cm^2 mmol^{-1}	$s_b \cdot 10^{-4}$ [b] cm^2 mmol^{-1}	a[c]	$s_{x,y} \cdot 10^3$[d]	$S \cdot 10^2$ [e] μg ml^{-1}
PAR[f]	495	7·55	0·03	0·190	4·36	0·78
	500	7·33	0·03	0·155	4·31	0·80
TAR[g]	540	3·86	0·01	0·237	2·90	1·52
	545	3·73	0·01	0·151	3·97	1·58
BrPADAP[h]	555	11·42	0·05	0·143	5·94	0·51
	560	11·46	0·06	0·116	7·41	0·50

[a] Regression straight line slope (approximate value of molar absorptivity); [b] standard deviation of slope; [c] displacement of regression straight line with standard deviation $s = 0{\cdot}003$; [d] standard deviation of dispersion about regression straight line $s_{y,x} = [\sum(A_{exp} - A_{calc})^2/(n-2)]^{1/2}$ (ref.[45]); [e] Sandell's sensitivity index[46] adapted for $A = 0{\cdot}01$; [f] $c_{Ni} = 0{\cdot}07-0{\cdot}65$ μg ml^{-1}, $c_L = 112$ μmol l^{-1}, pH 9·60 (0·1 mol l^{-1} borate buffer), number of experimental values $n = 20$; [g] $c_{Ni} = 0{\cdot}12 - 1{\cdot}45$ μg ml^{-1}, $c_L = 130$ μmol l^{-1}, pH 6·46 (0·2 mol l^{-1} ammonium acetate), 30 vol.% ethanol, $n = 22$; [h] $c_{Ni} = 0{\cdot}05 - 0{\cdot}49$ μg ml^{-1}, $c_L = 83{\cdot}6$ μmol l^{-1}, pH 7·50 (0·2 mol . l^{-1} TRIS), 10 vol.% ethanol, 0·1% BRIJ-35, $n = 25$.

in their spectral parameters. Their presence, however, has been assumed, similarly as in the case of the Mn(II) and Zn(II) complexes, from potentiometric measurements in 50 vol.% dioxane[14,15]. For PAR, and with a low degree of certainty for TAR, they could only be evaluated spectrophotometrically by computer processing (using the SPEFO 8 program) similarly as the ML_2H complexes in the systems of PAR with Zn(II), Cd(II) and Cu(II) (refs[47,48,22], respectively).

In the Ni(II)–BrPADAP system with excess reagent in 10 vol.% ethanol in the presence of 0·1% BRIJ-35, the NiL_2 species, in the presence of a smaller amount

TABLE XV

Effect of some ions on the determination of Ni(II) with BrPADAP. $c_{Ni} = 0{\cdot}296$ μg ml^{-1}, $c_L = 50$ μmol l^{-1}, pH 7·5 (0·2 mol l^{-1} TRIS), 10 vol.% ethanol containing 0·1% BRIJ-35, λ 560 nm

Ion	c_{ion} [a] μg ml^{-1}	m_{ion}/m_{Ni} [b]	Ion	c_{ion} [a] μg ml^{-1}	m_{ion}/m_{Ni} [b]
Fe^{3+}	0·028	0·95	Al^{3+}	54[c]	182
Co^{2+}	0·0059	0·020	Mg^{2+}	289	977
Cu^{2+}	0·0090	0·031	Ca^{2+}	160	542
Zn^{2+}	0·12[d]	0·41	Cl^-	355	1 198
Pb^{2+}	0·041	0·14	SO_4^{2-}	91	308

[a] Concentration bringing about a change in absorbance ($A - A_L$) of ±2% rel.; [b] mass ratio; [c] white haze appears immediately; [d] haze and colour change to yellow-brown appear in 30 min.

TABLE XVI

Effect of masking agents on the determination of Ni(II) with BrPADAP; $c_{Ni} = 5{\cdot}00$ μmol l^{-1}, $c_L = 50{\cdot}5$ μmol l^{-1}, pH 7·5 (0·2 mol l^{-1} TRIS), 10 vol.% ethanol containing 0·1% BRIJ-35, λ 560 nm

Masking agent	c [a] mmol l^{-1}	Masking agent	c [a] mmol l^{-1}
Mg^{2+}–EDTA	5	thiourea	100
EDTA	2[b]	tartrate	100
NaF	100	citrate	100
$Na_2S_2O_3$	20	oxalate	70

[a] Masking agent concentration bringing about a 2% decrease in absorbance of complex; [b] at $c_{Ni} = 6{\cdot}0$ μmol l^{-1} and pH 8·1 (0·2 mol l^{-1} TRIS).

TABLE XVII

Characteristics of Ni(II)–PAR and Ni(II)–TAR complexes in 30 vol.% ethanol and Ni(II)–BrPADAP complexes in 10 vol.% ethanol containing 0·1% BRIJ-35, $I = 0{\cdot}1$

Complex	λ_{max} nm	$\varepsilon(\lambda)$[a]	Equilibrium	log β	
				numerically	graphically
			PAR		
$NiLH^+$	510, 392	1·81(510)[b]	$M + L + H = MLH$	20·46	
		1·70(520)	$M + LH_3 = MLH + 2\,H$		−1·29[c]
			$M + LH = MLH$[d]	14·16	17·11[e]
NiL	493	4·20(490)[f]	$MLH = ML + H$		−6·56[g]
			$M + L = ML$	13·61	
$Ni(LH)_2$	520	3·39(520)	$M + 2\,L + 2\,H = M(LH)_2$	42·29	
		3·09(520)[h]	$M + 2\,LH = M(LH)_2$[d]	29·69	26·0[i]
NiL_2H^-[j]		5·77(520)	$M + 2\,L + H = ML_2H$	35·62	
			$M + LH + L = ML_2H$	29·32	
NiL_2^{2-}	490	7·96(490)[k]	$M + 2\,L = ML_2$	27·58	22·1[l]
			TAR		
$NiLH^+$	536, 415	2·18(540)	$M + L + H = MLH$	16·57	
		2·37(540)[m]	$M + LH_2 = MLH + H$		−0·70[n], −0·17[c]
		2·04(540)[o]	$M + LH = MLH$[d]	10·07	9·90[q], 9·25[p]
NiL	505	3·46(500)[r]	$MLH = ML + H$		−5·76[s], −5·47[t]
		2·30(540)	$M + L = ML$	11·08	10·0[o]
		2·1; 2·8(540)[o]			

$Ni(LH)_2$	540, 425	3·57(540)[r] 3·7(540)[o]	M + 2 L + 2 H = $M(LH)_2$ M + 2 LH = $M(LH)_2$	33·68 20·68	
NiL_2H^{-}[j]		4·43(540)[v]	M + 2 L + H = ML_2H M + LH + L = ML_2H	28·66 22·16	
NiL_2^{2-}		5·75(540)[v]	M + 2 L = ML_2 BrPADAP	21·00	17·1[x]
NiL	552, 525	4·82(560)	M + L = ML	13·04, 13·17[y]	
NiL_2	559, 525 560, 520	11·88(560) 12·6(560)[z]	M + 2L = ML_2	25·90, 26·11[y]	

[a] ε in 10^4 cm^2 $mmol^{-1}$ (average of values determined by SPEFO 8 program unless stated otherwise), λ in nm; [b] average of the values of $1{\cdot}80 \cdot 10^4$ and $1{\cdot}82 \cdot 10^4$ cm^2 $mmol^{-1}$ found by graphical analysis for $c_L = 50$ μmol l^{-1} and $c_M/c_L = 50$ and 100, respectively; [c] average of values found by graphical analysis for $c_L = 50$ μmol l^{-1} and λ 510 and 520 nm, log $\beta = -1{\cdot}28$ and $-1{\cdot}23$ ($c_M/c_L = 50$) and log $\beta = 1{\cdot}38$ and $-1{\cdot}28$ ($c_M/c_L = 100$); [d] the hypothetical LH^- species with dissociated *o*-OH group and undissociated *p*-OH group considered and the dissociation constant K_{a3} of the *o*-OH group used during the calculation of the stability constant (details see in ref.[22]); [e] value derived from the equilibrium constant $\beta([NiLH][H]^2/[Ni][LH_3])$, log $\beta = -1{\cdot}29$, determined by graphical analysis; [f] by graphical analysis at $c_L =$ $= 25{\cdot}0$ μmol l^{-1} and $c_M/c_L = 50$ and 100; [g] average of values found by graphical analysis at $c_L = 25{\cdot}0$ μmol l^{-1}, λ 480 and 490 nm, log $K_a =$ $= -6{\cdot}54$ and $-6{\cdot}55$ ($c_M/c_L = 50$) and $-6{\cdot}57$ and $-6{\cdot}56$ ($c_M/c_L = 100$); [h] from the horizontal segment of the pH curve as $(A - A_L)/c_M$ at $c_M = 7{\cdot}74$ μmol l^{-1}, $c_L/c_M = 10$, pH 4·0; [i] refs[13,14]; [j] λ_{max} not determined because of the formation of a mixture of complex species; [k] as *sub h* at pH 9—10; [l] ref.[11], average of values determined at excess reagent; [m] average of values determined by graphical analysis at $c_L =$ $= 40{\cdot}0$ μmol l^{-1}, λ 540 nm, $\varepsilon = 2{\cdot}38 \cdot 10^4$ ($c_M/c_L = 100$) and $2{\cdot}35 \cdot 10^4$ cm^2 $mmol^{-1}$ ($c_M/c_L = 200$); [n] average of values found by graphical analysis at $c_L = 40{\cdot}0$ μmol l^{-1}, log $\beta = -0{\cdot}55$, $-0{\cdot}67$ ($c_M/c_L = 100$, λ 500 and 540 nm, respectively) and $-0{\cdot}74$ ($c_M/c_L = 200$, λ 540 nm); [o] ref.[12]; [p] value derived from the equilibrium constant $\beta([NiLH][H]/[Ni][LH_2])$, log $\beta = -0{\cdot}65$; [q] average of values of 9·2 and 9·3, ref.[12]; [r] average of values found by graphical analysis at $c_L = 40{\cdot}0$ μmol l^{-1}, $\varepsilon = 3{\cdot}44 \cdot 10^4$ ($c_M/c_L = 100$) and $3{\cdot}48 \cdot 10^4$ cm^2 $mmol^{-1}$ ($c_M/c_L =$ $= 200$); [s] average of values found by graphical analysis at $c_L = 40$ μmol l^{-1}, log $K_a = -5{\cdot}70$ ($c_M/c_L = 100$) and $-5{\cdot}82$ ($c_M/c_L = 200$); [t] average of values of $-5{\cdot}44$ and $-5{\cdot}50$, ref.[12]; [v] average of values highly dispersed (Table VII) because of equilibrium overlap and occurrence of competitive equilibria; [x] average of values of 17·3 and 16·9, ref.[12]; [y] average of three values determined by SQUAD-G program for $c_L/c_M =$ $= 4{\cdot}64$; [z] ref.[20].

TABLE XVIII
Determination of Ni(II) with PAR, TAR and BrPADAP

Medium	pH	Buffer	c_L μmol l^{-1}	c_M μg ml^{-1}	Masking, separation of interferents	λ nm	ε . 10^{-4} cm^2 $mmol^{-1}$	Application	Ref.
Water	4·3	acetate	110	0·1—0·9	EDTA, thiourea, ascorbic acid	525[a]	5·2	Cu–Ni–Pd alloys	3
Water	4·5	acetate pH 4	84		thiourea	570[a]		tungsten	4
Acetone 40 vol.%	4—5	—	48	0·096	thiourea, citrate	540[a]	3·2	cast iron, low-alloy steels	5
Chloroform (extraction)	9·3—9·5	tetraborate	42	0·2—5 μg	3-methylglyoxime (Co(II))	500[b]	8·08	crude oil	8
Water	9·2	borate			separation of Ni(II)–PAR complex[c]	496[d]		steel	6
Water	7·95—9·85	borate	40		EDTA, Dowex 1X10 (Fe, Co, UO_2)	496[d]		mineral waters	2

Water	8·6—10	borate pH 9·3	840	0·05—1·0	EDTA, fluoride, citrate	494[d]	7·3	pure solutions	9
Water	9·2—10·0	borate pH 9·6	110	0·07—0·65	EDTA citrate, thiourea, Dowex 1X8[e]	495	7·96	drinking water	this work
				TAR					
Ethanol 30 vol.%	6·0—7·0	ammonium acetate pH 6·5	130	0·1—1·45	—	540[f]	3·86	pure solutions	this work
				BrPADAP					
Ethanol 50 vol.%	5—10	acetate pH 5·5	46	0·6	metaphosphate, thiosulphate fluoride	560[d]	12·6	aluminium alloys *etc.*	20
Ethanol 10 vol.%, BRIJ-35 0·1%	6·5—9·0	TRIS pH 7·5	84	0·05—0·49	EDTA, citrate, thiourea, fluoride	560[d]	12·1	pure solutions	this work

[a] $Ni(LH)_2$ complex; [b] Ni(II)–PAR–tetradecyldimethylbenzylammonium chloride ($2Q^+.NiL_2^{2-}$) ternary complex; [c] by extraction into ethyl acetate at pH 4; [d] NiL_2 complex; [e] for the separation of transition metals; [f] the NiL_2H complex predominates beside small quantities of $Ni(LH)_2$ and NiL_2.

of NiL, was found by the SQUAD-G and SPEFO 8 programs. The average ε and $\log \beta$ values of the complexes found by the SPEFO 8 program at 560 nm and the rather approximative estimates determined by the SQUAD-G program at 22 wavelengths within the region of 380–580 nm are given in Table XVII.

When comparing the results of graphical and numerical data treatment for both the Ni(II)–PAR and Ni(II)–TAR systems, it is observed that appreciably erroneous values of the constants are attained by the graphical treatment if the simultaneous formation of several complexes is ignored (*e.g.*, the stability constants of the NiLH and NiL_2 complexes of PAR or the NiL and NiL_2 complexes of TAR, Table XVII). The computer processing, however, did not invariably lead to unique correct results either. When testing the adequacy of the various conceivable complexation equilibria models, even the optimum models frequently displayed, besides $\sigma(A)$ values roughly corresponding to the accuracy of data measured (several thousandths in the absorbance scale), increased $\sigma(A)$ values (as high as 0·02). The poor reproducibility of $\sigma(A)$ then made it more difficult to recognize the correct model, particularly if several models provided $\sigma(A)$ values not very different from each other (Tables II, VI, X).

Particularly difficult and uncertain was the discrimination betwen the model of NiLH, NiL, $Ni(LH)_2$, NiL_2 and the same model with NiL_2H for TAR. For either of them the $\sigma(A)$ values were relatively low, and neither could be rejected based on anomalies in the parameter values – the ε and $\log \beta$ values and the corresponding standard deviations were at reasonable levels.

For the Ni(II)–BrPADAP system ,more accurate results could be potentially gained than for the Ni(II)–PAR and Ni(II)–TAR systems owing to the fact that a more perfect instrumentation was used (Superscan 3 interfaced to a HP 9815 computer), the σ(A) values, however, apparently involved other errors arising from the properties of this system, such as the tendency of the low-soluble reagent and complexes to form colloid particles, high sensitivity and low selectivity of the reagent during its reactions with metal ions which may be present as impurities in the chemicals, *etc.* All data available, such as the absorption spectra, results of the method of continuous variations, ε estimates derived from the horizontal branches of the pH and concentration dependences, partial results of graphical analysis, data from the literature, *etc.*, had therefore to be taken into consideration, and were found relevant, when seeking for the optimum model.

In the final numerical evaluation of the optimum models in conditions of a simultaneous formation of complexes with similar absorption spectra, the precision of the data measured was not sufficient for the ε and β values of some complexes to be determined reliably enough; this concerns, *e.g.*, the PAR and TAR complexes with M : L = 1 : 2 or, in particular, the NiL complex of BrPADAP when employing the SQUAD-G program and data from a wider wavelength region where competitive equilibria interfere to a higher extent. The optimum conditions for the suggested

methods of determination of Ni(II) with PAR, TAR and BrPADAP, respectively, are given in Table XVIII.

The various procedures for the determination of Ni(II) with PAR differ particularly in the suggested concentrations of reagent, which, however, according to the response surface (Fig. 4) all are sufficient for a quantitatie formation of the $Ni(LH)_2$ complex at pH 4·5 and the NiL_2 complex, with a higher molar absorptivity, at pH 9–10. The latter complex was used in this work for the determination of Ni(II) in drinking water.

TAR as a reagent for the spectrophotometric determination of Ni(II) in 30 vol.% ethanol at pH 6·0–7·0 is less suitable than PAR because of the lower sensitivity of determination, partial dissociation of the complexes and a marked increase in the absorbance of reagent at pH > 7.

With BrPADAP, featuring an exceedingly high sensitivity ($\varepsilon_{560} = 1{\cdot}21 \cdot 10^5$ cm^2 . . mmol^{-1}), the possibility of determination of Ni(II) was tested in 10 vol.% ethanol containing 0·1% BRIJ-35 tenside; the determination, however, was found little selective, calling for masking or, better, previous separation of interfering ions.

REFERENCES

1. Ivanov V. M.: *Geterotsiklicheskie azotsoderzhashchie azosoedineniya*, p. 148. Nauka, Moscow 1982.
2. Nevoral V., Okáč A.: Cesk. Farm. *17*, 478 (1968).
3. Volkova M. P., Kolesnikov B. P., Kossykh B. G.: Zh. Anal. Khim. *32*, 2139 (1977).
4. Chelnokova M. N., Bredneva L. G., in ref.[1], p. 151.
5. Pilipenko A. T., Dyachenko N. A.: Ukr. Khim. Zh. *49*, 269 (1983).
6. Nonova D., Lichareva N.: C. R. Acad. Bulg. Sci. *27*, 815 (1974).
7. Hoshino H., Yotsuyanagi T., Aomura K.: Anal. Chim. Acta *83*, 317 (1976).
8. Yotsuyanagi T., Yamashita R., Hoshino H., Aomura K., Sato H., Masuda N.: Anal. Chim. Acta *82*, 431 (1973).
9. Shijo Y., Takeuchi J.: Jpn. Analyst *14*, 511 (1965); Anal. Abstr. 1967, 1422.
10. Iwamoto T.: Bull. Chem. Soc. Jpn. *34*, 605 (1961).
11. Nonova D., Evtimova B. E.: Anal. Chim. Acta *62*, 456 (1972).
12. Mushran S. P., Sommer L.: This Journal *34*, 3693 (1969).
13. Corsini A., Yih M. L., Fernando G., Freiser H.: Anal. Chem. *34*, 1090 (1962).
14. Corsini A., Fernando Q., Freiser H.: Inorg. Chem. *2*, 224 (1963).
15. Stanley R. W., Cheney G. E.: Talanta *13*, 1619 (1966).
16. Navrátil O.: This Journal *41*, 2682 (1976).
17. Macka M., Kubáň V.: This Journal *47*, 2676 (1982).
18. Kubáň V., Macka M.: This Journal *48*, 52 (1983).
19. Navrátilová-Ševčíková R., Jančář L., Sommer L.: Scripta Fac. Sci. Nat. Univ. Purkyně Brno *15*, No. 9–10 (Chemia), 505 (1985).
20. Wei F. S., Qu P. H., Shen N. K., Yin F.: Talanta *28*, 189 (1981).
21. Zhou T., Xie Y., Qin X., Dai S.: Huaxue Shiji *1982*, 182; Chem. Abstr. *97*, 229281t (1982).
22. Hrdlička A., Langová M.: This Journal *45*, 1502 (1980).
23. Havel J.: This Journal *62*, 1250 (1968).

24. Kubáň V., Havel J., Sommer L.: This Journal *30*, 604 (1975).
25. Voznica P., Havel J., Sommer L.: This Journal *45*, 54 (1980).
26. Sommer L., Kubáň V., Havel J.: Folia Fac. Sci. Nat. Univ. Brunensis *11*, Chemia *7*, 1 (1970).
27. Suchánek M., Šůcha L.: Sb. Vys. Sk. Chem.-Technol. Praze H *13*, 41 (1978).
28. Koblížková V., Kubáň V., Sommer L.: This Journal *43*, 2711 (1978).
29. Sommer L., Havel J.: This Journal *42*, 2134 (1977).
30. Sillén L. G.: Acta Chem. Scand. *16*, 159 (1962); 18, 1085 (1964).
31. Ingri M., Kakolowicz W., Sillén L. G., Warnqvist B.: Talanta *14*, 1261 (1967).
32. Pavlíková M.: *Thesis*. Purkyně University, Brno 1976.
33. Havel J.: Scripta Fac. Sci. Nat. Univ. Purkyně Brno *3*, Chemia 4, 117 (1973).
34. Legget D. J., Mc Bryde W. A. E.: Anal. Chem. *47*, 1065 (1975).
35. Jančář L., Havel J.: Scripta Fac. Sci. Nat. Univ. Purkyně Brno *14*, Chemia 3—4, 73 (1984).
36. Box G. E. P.: Biometrics *10*, 16 (1954).
37. Frazer J. W., Ridgon L. P., Brand H. R., Pomernacki C. L.: Anal. Chem. *51*, 1747 (1979).
38. Otto M.: Z. Chem. *23*, 204 (1983).
39. Ruseva E., Kubáň V., Sommer L.: This Journal *44*, 374 (1979).
40. Kragten J.: *Atlas of Metal Ligand Equilibria in Aqueous Solutions*, p. 508. Ellis Horwood, Chichester 1979.
41. Hátle J., Likeš J.: *Základy počtu pravděpodobnosti a matematické statistiky*, p. 389. Published by SNTL, Prague 1980.
42. Slováková S., Slovák Z.: Anal. Chem. *292*, 213 (1978).
43. Johnson D. A., Florence T. M.: Talanta *22*, 253 (1975).
44. Macka M., Kubáň V.: This Journal *47*, 2676 (1982).
45. Eckschlager K., Horsák I., Kodejš Z.: *Vyhodnocování analytických výsledků a metod*, p. 86. Published by SNTL, Prague 1980.
46. Sandell E. B.: *Colorimetric Determination of Traces of Metals*, p. 218. Interscience New York—London 1959.
47. Pollak M., Kubáň V.: This Journal *44*, 725 (1979).
48. Vlčková S., Jančář L., Kubáň V., Havel J.: This Journal *47*, 1086 (1982).

Translated by P. Adámek.